

Thermal Traits Vary with Mass and across Populations of the Marsh Periwinkle, *Littoraria irrorata*

REBECCA L. ATKINS*, KATHLEEN M. CLANCY, WILLIAM T. ELLIS,
AND CRAIG W. OSENBERG

Odum School of Ecology, University of Georgia, 140 East Green Street, Athens, Georgia 30602

Abstract. Physiological processes influence how individuals perform in various environmental contexts. The basis of such processes, metabolism, scales allometrically with body mass and nonlinearly with temperature, as described by a thermal performance curve. Past studies of thermal performance curves tend to focus on effects of temperature on a single body size or population, rather than variation in the thermal performance curve across sizes and populations. Here, we estimate intraspecific variation in parameters of the thermal performance curve in the salt marsh gastropod *Littoraria irrorata*. First, we quantify the thermal performance curve for respiration rate as a function of both temperature and body size in *Littoraria* and evaluate whether the thermal parameters and body size scaling are interdependent. Next, we quantify how parameters in the thermal performance curve for feeding rate vary between three *Littoraria* populations that occur along a latitudinal gradient. Our work suggests that the thermal traits describing *Littoraria* respiration are dependent on body mass and that both the thermal traits and the mass scaling of feeding

vary across sites. We found limited evidence to suggest that mass scaling of *Littoraria* feeding or respiration rates depends on temperature. Variation in the thermal performance curves interacts with the size structure of the *Littoraria* population to generate divergent population-level responses to temperature. These results highlight the importance of considering variation in population size structure and physiological allometry when attempting to predict how temperature change will affect physiological responses and consumer-resource interactions.

Introduction

An individual's fitness is the result of a suite of performance metrics (*e.g.*, growth, fecundity, mobility, *etc.*) that are often mediated by effects on the individual's energy metabolism (Sinclair *et al.*, 2016). The metabolic theory of ecology (MTE) posits that metabolism is a nonlinear function of both mass and temperature (Brown *et al.*, 2004):

$$b(M, T) = b_0 M^\alpha e^{\frac{E_a}{k}(\frac{1}{T_c} - \frac{1}{T})}, \quad (1)$$

where $b(M, T)$ is the metabolic rate of an organism of mass M at temperature T (in degrees Kelvin), b_0 is the metabolic rate of a 1-unit mass individual at an arbitrary reference temperature (T_c), M is body mass, α is the allometric mass-scaling exponent (usually around 3/4), E_a is the activation energy of the metabolic process (in electron volts, assumed to approximately equal 0.65 eV for processes governed by respiration: Gillooly *et al.*, 2001; Brown *et al.*, 2004), and k is Boltzmann's constant (8.62×10^{-5} eV K⁻¹). The application of equation 1 represents that there is a single rate-limiting step constraining metabolism and that metabolism increases monotonically with increasing temperature (DeLong *et al.*, 2017).

Responses of metabolism and other processes to temperature are often better described by unimodal thermal performance curves (TPCs) that increase up to a maximum (which

Received 16 December 2020; Accepted 7 March 2022; Published online 20 May 2022.

* To whom correspondence should be addressed. Email: atkinsr@uga.edu.

Abbreviations: α , mass-scaling exponent; AIC_c, Akaike information criterion for small sample sizes; β_x , the slope of the relationship between parameter x and temperature (T) or mass (M), that is, the parameter that controls the temperature or mass dependency of parameter x ; b_0 , the respiration or feeding rate of a 1-unit mass individual at a reference temperature (T_c); b_{max} , an individual's peak rate of respiration occurring at T_{opt} ; $b(M, T)$, an individual's rate of respiration at mass (M) and temperature (T); BIC, Bayesian information criterion; c , controls the width of the thermal performance curve; CI, confidence interval; E_a , enzyme activation energy; E_h , high-temperature enzyme deactivation energy; FL, Florida collection site; M , an individual's dry tissue mass (mg); MTE, metabolic theory of ecology; SC, South Carolina collection site; T_c , reference temperature (which we set to 298.15 °K [25 °C]); T_h , temperature at which half the enzymes are no longer functional; T_{opt} , temperature at which a trait (respiration or feeding rate) is maximal; TPC, thermal performance curve; VA, Virginia collection site; x' , the intercept value of parameter x as a function of temperature (T) or mass (M).

we call T_{opt}) and then decline as a result of inactivation of enzymes (Dell *et al.*, 2014). Examples include the Sharpe-Schoolfield (Sharpe and DeMichele, 1977; Schoolfield *et al.*, 1981), macromolecular rate (Hobbs *et al.*, 2013), and enzyme-assisted Arrhenius (DeLong *et al.*, 2017) models. For example, Schaum *et al.* (2018) combined the Sharpe-Schoolfield equation with body mass scaling to predict metabolism as a function of mass and temperature:

$$b(M, T) = \frac{b_0 M^\alpha e^{\frac{E_a}{k}(\frac{1}{T_c} - \frac{1}{T})}}{1 + e^{\frac{E_h}{k}(\frac{1}{T_h} - \frac{1}{T})}}, \quad (2)$$

where E_a describes the upward slope of the curve due to enzyme activation (as in equation 1), E_h describes the downward slope due to enzyme deactivation, T_h is the temperature at which half the enzymes are no longer functional, and other parameters are as defined above. In this model, T_{opt} is not an explicit parameter but instead emerges from the others.

Because of its complexity, the modified Sharpe-Schoolfield model can be easily overfit with smaller datasets (Angilletta, 2006). One potential solution to reduce this risk is to compare these complex models with simpler, but widely used, models such as the Gaussian function (Lynch and Gabriel, 1987):

$$b(M, T) = b_{max} M^\alpha e^{-\left(\frac{T - T_{opt}}{2c}\right)^2}, \quad (3)$$

where b_{max} is the organism's peak rate of respiration occurring at T_{opt} and c controls the width of the curve. As with the Sharpe-Schoolfield model, this model incorporates the effect of mass M (in milligrams dry mass) on respiration *via* the allometric scaling exponent, α , and assumes that respiration is a unimodal function of temperature. The Gaussian model is symmetric with temperature and cannot re-create the asymmetry arising from the E_a and E_h parameters in the Sharpe-Schoolfield model. While the Gaussian model is not designed to convey any underlying mechanisms, it holds two advantages over the Sharpe-Schoolfield model: it has one fewer parameter, and the temperature at which b is maximized (T_{opt}) is a parameter (rather than emerging indirectly from the other parameters).

Interspecific variation in thermal performance suggests that there is selection on thermal traits, such as the parameters in equation 2 (Padfield *et al.*, 2016). Thermal tolerance in ectotherms generally suggests a limited capacity for change in upper thermal limits in terrestrial, but not marine, species (Sunday *et al.*, 2011). Furthermore, in accordance with the climate extremes hypothesis, thermal tolerance increases in more thermally variable environments (Sunday *et al.*, 2019). Complex patterns have also been observed between latitude, T_{opt} , and peak metabolic performance (*e.g.*, "hotter is better" hypothesis; Clarke, 1993; Kingsolver and Huey, 2008; Angilletta *et al.*, 2010; DeLong *et al.*, 2018). Most of these inter-

specific comparisons of thermal responses assume that intraspecific variation in TPCs (and their associated parameters) is minimal (Sinclair *et al.*, 2016).

However, empirical studies suggest that intraspecific variation can be considerable and affected by a range of factors including, but not limited to, developmental temperature (Hoefnagel and Verberk, 2017), latitude (Gaitán-Espitia *et al.*, 2013, 2014), predation (Luhring and DeLong, 2016), trophic structure (Garzke *et al.*, 2019), microgeographic gradients in temperature (Tüzün *et al.*, 2017), environmental heterogeneity (Stager *et al.*, 2021), life stage (Kingsolver *et al.*, 2011), temporal shifts in temperature (Domínguez-Guerrero *et al.*, 2020; but see Wooliver *et al.*, 2020), and thermoregulatory behavior (Miller and Denny, 2011). Despite this knowledge, relatively few studies link this intraspecific variation in thermal performance to parameterization of TPCs (such as equation 2).

The application of TPCs can provide insight about the sources of variation in thermal performance. A handful of studies demonstrate shifts in thermal tolerance and maximum performance as a function of body size (Klockmann *et al.*, 2017; DeLong *et al.*, 2018; Franken *et al.*, 2018; Truebano *et al.*, 2018; Leiva *et al.*, 2019; Johnson and Stahlschmidt, 2020). However, few directly assess whether the temperature at which performance is maximal (which we refer to as T_{opt} to avoid confusion with the critical upper thermal limit, often referred to as T_{max}) varies intraspecifically with mass (but see evidence of shifts across ontogeny in Kingsolver *et al.*, 2011; Rebolledo *et al.*, 2020). However, T_{opt} (either as a parameter in equation 3 or inferred from the other parameters in equation 2) is independent of body mass, so these observed differences in T_{opt} between size classes must be due to more than a simple body size effect. One possibility is that the thermal traits (E_a , E_h , or T_h in equation 2, or T_{opt} in equation 3) might not be constants but might instead be functions of body size. In such cases, T_{opt} could vary between different size classes, and the cause of this effect (*e.g.*, *via* changes in E_a , E_h , or T_h ; see Fig. A1) could give insight into the underlying mechanisms or biochemical pathways. However, these possible interactions between body size and thermal traits are generally not considered in studies of thermal performance. The effects of mass on thermal traits are particularly relevant in size-structured populations because variation in size structure, combined with size-dependent thermal traits, will alter how a population responds to an environmental change (Dunham *et al.*, 1989).

Alternatively, the effect of body size (as reflected in the value of α in equations 2 and 3) might depend on temperature. A handful of studies have documented an interaction between temperature and mass scaling, although the effect is variable: α can decrease, increase, or not change with temperature (Newell, 1973; Xiaojun and Ruyung, 1990; Glazier, 2005; Ohlberger *et al.*, 2012; Carey and Sigwart, 2014; Lindmark *et al.*, 2018; Rubalcaba *et al.*, 2020). For example, Carey and Sigwart (2014) found that as temperature increased, the mass-scaling exponent (α) of three chiton species decreased

linearly so that metabolic rates of smaller individuals rose more with increased temperatures than was observed for larger individuals. These findings suggest that smaller individuals were more responsive to warming temperatures (*i.e.*, temperature had a stronger stimulatory effect on metabolism in smaller animals). Varying sensitivity to temperature between size classes could in part be explained by the metabolic level boundaries hypothesis (*i.e.*, constraints due to activity level; Glazier, 2010; Ohlberger *et al.*, 2012), size-specific variation in microclimates (Kingsolver *et al.*, 2011), or ontogenetic shifts in energetic allocation to physiological pathways related to heat stress (*e.g.*, heat-shock protein expression; Ueda and Boettcher, 2009; Cottin *et al.*, 2015).

Differences in physiological rates owing to mass-temperature interactions have the potential to scale up to alter population-level energy requirements and the strength of species interactions (*e.g.*, between consumers and their resources). For example, modeling stage-structured fish populations, Lindmark *et al.* (2018) demonstrated how temperature-dependent intraspecific allometry in metabolic rates can alter population regulation and dynamics *via* shifts in the competitive dominance of different life stages. Investigating intraspecific variation in the effect of temperature on ectotherm performance (*e.g.*, feeding and respiration), due to both body size and between-population variation, could potentially improve our predictions of population response to changing temperatures (Monaco *et al.*, 2019).

Using the salt marsh periwinkle, *Littoraria irrorata* (Say, 1822), this study aims to (1) compare the fit of two functions, Gaussian and Sharpe-Schoolfield, commonly applied to thermal performance metrics; (2) determine whether thermal performance traits associated with respiration and feeding rates in *Littoraria* differ across body sizes (*i.e.*, whether the parameters that govern thermal responses depend on body mass); (3) determine whether the scaling effects of body mass on respiration and feeding rates depend on temperature (*i.e.*, temperature-dependent mass scaling); (4) determine whether the thermal performance traits associated with feeding rate vary across populations; and (5) integrate this information to quantify how population-level metabolism varies in response to shifts in size structure and temperature. We conducted our investigations by using 3 size classes of *Littoraria* from 3 sites spanning 7 degrees of latitude.

Littoraria irrorata is an herbivorous ectotherm that occurs throughout west Atlantic marshes (Pennings and Silliman, 2005). After a planktonic larval stage, *Littoraria* settles into the furled leaves of *Spartina alterniflora*, the dominant marsh grass, until reaching a shell height of 4–6 mm in length (Pennings *et al.*, 2016). Over a decade, it can attain shell heights upward of 20 mm (Stiven and Hunter, 1976). Within and across marshes, the size structure of *Littoraria* varies due to ecological factors, such as predation, resources, and elevation (Stanhope *et al.*, 1982; Stagg and Mendelssohn, 2012). This variation in body size, combined with variation in density, causes

variation in the metabolic biomass of *Littoraria* populations; this variation has significant effects on the magnitude and direction of the *Littoraria-Spartina* interaction (Silliman and Ziemann, 2001; Atkins *et al.*, 2015). For example, at extremely high densities, *Littoraria* populations can exacerbate environmental stressors like drought, almost completely denuding above-ground plant biomass (Silliman, 2005). *Littoraria* can also experience large shifts in temperature over small spatial and temporal scales. For example, *Littoraria* body temperatures in a South Carolina marsh were recorded to range from 17 °C to 48 °C within a single week; body temperature differences can also exceed 5 °C across 20 cm of vertical height along *Spartina* stems (Iacarella and Helmuth, 2011). Because of variation in body size between sites, and the differential effects of large *versus* small snails on plants, future temperature change will likely alter the interactions between snails and *Spartina*, driven, in part, by effects of temperature and body size on feeding rates and energy requirements.

Materials and Methods

Respiration experiment: collection and study site

To quantify TPCs for respiration, we collected *Littoraria* Gray, 1833 from a Florida salt marsh (30.016745 °N, –81.344573 °W) located within the Guana Tolomato Matanzas National Estuarine Research Reserve (NERR) on February 25, 2018, and transported specimens (within eight hours of collection) to a laboratory at the University of Georgia in Athens. During transportation, *Littoraria* specimens were housed in a single bin containing mud and *Spartina alterniflora* Loisel. stalks clipped from the collection site to serve as both a natural climbing structure and a food source. No seawater was added to the bins, although *Littoraria* specimens were misted with freshwater to prevent desiccation. Average daily air temperature across the month of February 2018 at the collection site was about 18.1 °C ± 3.0 °C (mean ± SD) (Weather Underground, 2018). Air temperatures are particularly relevant to the physiology of *Littoraria* because individuals exhibit climbing behaviors to avoid being submerged and vulnerable to nektonic predators during the high tide (Hamilton, 1977; Vaughn and Fisher, 1992). Because of this, we based our laboratory acclimation temperature on ambient air temperature rather than water temperature. Upon reaching Athens, we placed this bin in a Percival incubator (model I-30VL, Percival Scientific, Fontana, WI) programmed to a 12h:12h light:dark cycle (6 a.m. to 6 p.m.) at 18 °C and allowed snails to acclimate for 12 hours. Temperature in the incubator was then increased to 21 °C (beginning at 6:30 a.m.) for 24 hours and then to the final acclimation temperature of 25 °C (beginning at 6:30 a.m. on February 27). We chose this temperature because it is within the thermo-neutral zone of *Littoraria* (*e.g.*, Shirley *et al.*, 1978), and it facilitated comparisons with planned studies that would be conducted at that acclimation temperature in the future.

This temperature also served as our reference temperature (T_c) when fitting the Sharpe-Schoolfield model. Respiration trials began on March 1.

For this experiment and the feeding experiment (see below), we converted shell height to mass based on shell height-dry mass regressions, using *Littoraria* collected from the Florida site (and also from the Virginia and South Carolina marshes) in August 2018 as part of the feeding experiment. Using *Littoraria* collected from the three sites, we measured shell height (Fig. A2), removed the shell, dried the tissue and operculum at 60 °C for 72 hours, and weighed each snail to obtain shell-free dry mass. The resulting regression equations for each site (Fig. A2) were applied to each snail used in the experiment to estimate its dry mass. Although we applied separate regressions to different sites, we did not distinguish sexes because there is no support for sex-specific allometry in *Littoraria* (Bistransin, 1976; Rietl *et al.*, 2018). In addition, all individuals used in this study were likely reproductively mature (shell height >6 mm; Bingham, 1972), further reducing within-site variation.

Respiration experiment: experimental design

We set up a Picarro gas concentration analyzer (G2401, Santa Clara, CA) with a closed-loop chamber system that continuously measured and recorded CO₂ in parts per million in one- to two-second intervals. We attached the ends of the loop through the lid of a 250-mL glass jar that would serve as the respirometry chamber and house a single study organism. The metal lid was custom fabricated to create an airtight seal with the loop and was secured to the jar by using a metal screw band and silicone ring gasket. We placed this jar inside a Percival incubator (model I-30VL) that we used to manipulate temperature. To avoid desiccation, we put 5 mL of salt-water made from Instant Ocean sea salt (Spectrum Brands, Blacksburg, VA) into the jar before each trial and lowered a mesh cap into the jar to prevent *Littoraria* from climbing up the side of the jar.

At least one day prior to starting trials, we cleaned the surface of each *Littoraria* shell, using a bleach solution to minimize the possible contribution of epiphytic or microbial respiration within the jar, and then individually labeled each shell with permanent marker. We measured all shells from the base to the tip of the spire by using an electronic caliper (Fig. A2). Last, to obtain a range of body sizes, we categorized all *Littoraria* by size class: large (20.13 ± 1.02 mm shell height; 88.31 ± 13.98 mg dry mass), medium (14.14 ± 0.52 mm; 30.44 ± 3.33 mg), and small (8.95 ± 0.96 mm; 7.88 ± 2.56 mg) (mean \pm SD) (Fig. A3). At these sizes, individuals occupied about 0.08%–3% of the respirometry chamber volume.

Twenty-four hours before each trial began, we removed one *Littoraria* of each size class from the original bin and placed it into a holding container with only Instant Ocean, about 2 mm deep (*i.e.*, no food was present). Each day, we

ran three trials, one for each size class, the order of which was randomly determined. At the start of the first trial, we placed the snail of the appropriate size class in the Picarro respirometry chamber at 25 °C for 30 minutes. Temperature in the incubator was programmed to lower 5 °C every 30 minutes to allow the air circulating within the closed-loop system time to mix. The trial period began when the incubator temperature reached 15 °C (about 1 hour after the *Littoraria* had been placed in the chamber), at which point temperatures were gradually increased to 50 °C in 5 °C increments every 30 minutes (for a total of eight temperatures; Table A1). The 15 to 50 °C range represents an ecologically relevant range of temperatures: lethal limits for *Littoraria* are around 45 °C (Bingham, 1972; Iacarella and Helmuth, 2011), and the lower threshold at which *Littoraria* transitions into dormancy is about 10 to 15 °C (Bingham, 1972; Paul *et al.*, 1989). At the end of the trial, we removed the *Littoraria* individual, set the incubator temperature to 25 °C, and placed the next snail of a different size class into the test chamber. We repeated the procedure for this snail and then the third snail. Thus, three trials were run on each of eight days, using the same trial schedule (trials beginning at about 8:30 a.m., 1:30 p.m., and 6:30 p.m.), although we varied the order of size classes to avoid any confounding that might have been caused by diurnal metabolic rhythms (Shirley and Findley, 1978; Shirley *et al.*, 1978). We did not run any trials using an empty jar, so we assume that background gas exchange was minor and consistent across all trials.

Acclimation duration and temperature can influence traits like thermal tolerance (*e.g.*, thermal breadth), and the plasticity of these traits is known to differ across taxa (Gunderson and Stillman, 2015) and between animals of different body sizes (Rohr *et al.*, 2018). Previous experiments using *Littoraria* vary greatly in their acclimation times, ramping rates, and measurement duration, but little is known about how such procedural differences affect measured rates. While one study of two Atlantic intertidal littorinid species suggests that large daily temperature fluctuations under field conditions suppress the capacity for respiratory temperature acclimation (McMahon *et al.*, 1995), seasonal respiration rates in *Littoraria* are suggestive of cold temperature acclimation (Shirley *et al.*, 1978). Thus, feeding and respiration responses measured in this experiment should be considered acute responses to temperature (Henry *et al.*, 1993).

To evaluate the temporal pattern of body temperatures during our experimental protocol, we conducted an additional trial using *Littoraria* shells filled with silicone, which have been shown to adequately mimic the thermal properties of living *Littoraria* (Iacarella and Helmuth, 2011). We inserted T-type thermocouple sensors into the aperture of each shell before injecting silicone and then allowed the silicone to cure for 48 hours. Each biomimic was placed in a 250-mL jar with 5 mL of freshwater. The top of each jar was sealed with Sculpltex modeling clay (Reynolds Advanced Materials,

Detroit, MI) to prevent gas exchange between the jar and the Percival incubator. We used the same three size classes of *Littoraria* replicated five times. All individuals were measured simultaneously using a T-type Arduino thermocouple multiplexer shield (Somerville, MA). Although we did not collect data on thermoregulatory behavior during trials with live snails, we know from Iacarella and Helmuth (2011) that evaporative cooling behaviors reduce the body temperatures of *Littoraria* by only about 1 °C.

Respiration experiment: analysis

Trials using the silicone models confirmed that body temperatures across our 3 size classes changed uniformly across the ramping trial and were invariant during the last 15 minutes of each 30-minute temperature period (Fig. A4).

Respiration data from the live snails were downloaded from Picarro and imported into RStudio (RStudio Team, 2020). Respiration rates were calculated as the slope of a linear regression of CO₂ (ppm) through time during the last 15 minutes of each 30-minute temperature period (*i.e.*, after body temperatures had stabilized). A total of 192 respiration rates were obtained for the 24 snails: 8 replicates (*i.e.*, 8 days) × 3 size classes × 8 temperatures (Fig. A3). Respiration rates below zero were sometimes estimated, especially for the smallest snails; this could reflect a combination of measurement error, the low respiration rates in smaller snails, and possible photosynthesis (although trials were run in low light conditions). We fit models with these negative estimates to avoid biasing results (which would occur if we truncated the observations to be >0).

Because of the complexity of the design and the Sharpe-Schoolfield model, we took a sequential approach to our analysis. First, we explored the role of snail ID as a random effect in the Sharpe-Schoolfield model. We found limited support for between-snail variation in thermal traits, so we did not consider random effects further.

We fit the modified Sharpe-Schoolfield (equation 2) and Gaussian (equation 3) models to the data, using the generalized non-linear least squares regression (gnls function in the nlme package for R, package ver. 3.1-152; Pinheiro *et al.*, 2021), which allowed for unequal variance. We assumed that variances increased exponentially with mass. We tested for mass dependencies of thermal traits (*i.e.*, E_a , E_h , and T_h in the Sharpe-Schoolfield model and T_{opt} and c in the Gaussian model) by comparing the null model that lacked mass dependencies (constant values of the thermal traits) with models representing the seven combinations (for the Sharpe-Schoolfield) or three combinations (for the Gaussian) of potential mass-dependent thermal traits. We modeled the mass dependencies by including a linear effect of mass on each thermal trait (*e.g.*, $E_a = E_a^l + \beta_{E_a}M$, where β_{E_a} is the parameter that controls the mass dependency of E_a). Here, and subsequently, we compared models using the Bayesian information criterion (BIC function within the lme4 package ver. 1.1-23; Bates *et al.*,

2015) and selected the model with the lowest BIC. In addition to reporting BIC, we also report the Akaike information criterion for small sample sizes (AIC_c function within the MuMIn package ver. 1.43.17; Bartoń, 2020) and likelihood ratio tests to assess the fit of nested models (function anova within the stats package ver. 4.0.4; R Core Team, 2021). We then compared the best model (lowest BIC) with one that also incorporated a temperature dependency on the mass scaling (*i.e.*, assuming a linear relationship between the mass-scaling parameter, α , and temperature, T : $\alpha = \alpha' + \beta_{\alpha}T$). For the Sharpe-Schoolfield model, T_{opt} was estimated by fitting the model with the lowest BIC across a range of temperatures (15 to 50 °C) and calculating the temperature at which respiration was maximal. We report the 95% confidence intervals (CIs) for the parameter estimates for the best model using the confint function in the MASS package version 7.3-54 (Venables and Ripley, 2002). Throughout, we fit the Sharpe-Schoolfield and Gaussian models by using temperature in Kelvin and Celsius, respectively (and mass in milligrams dry mass), but for presentation purposes we present all temperatures in degrees Celsius.

Confidence intervals around the TPCs were generated with bootstrapping, in which we resampled the data (with replacement), refit the model, and obtained new parameter estimates for the simulated datasets (using the boot_nlme function within the nlraa package ver. 0.98; Miguez, 2021). Using each of the 500 resampled datasets and associated parameter estimates, we calculated the predicted respiration of a small, medium, and large snail (using the median mass for each size class) across the temperature gradient (15 to 50 °C) and estimated the 95% CI, using the 2.5% and 97.5% quantiles of these calculated respiration rates at each combination of temperature and size class. Bootstrapping was also used to obtain size class-specific estimates of T_{opt} for both TPC functions.

Feeding experiment: collection and study site

To assess whether TPCs for feeding rates varied between populations and to assess whether thermal traits and body size scaling interact, we collected *Littoraria*, as well as *Spartina*, from three salt marshes: one in Florida (FL: 30.016745 °N, -81.344573 °W) on August 16 (the same one used for the respiration experiment), one in South Carolina (SC: 33.333870 °N, -79.197500 °W) on August 16, and one in Virginia (VA: 37.320154 °N, -76.280907 °W) on August 17, 2018. Snails were haphazardly collected from an area of each marsh coinciding with their peak population densities. Areas where densities are highest also tended to include a more complete representation of the size spectrum, thus allowing us to collect individuals of different sizes from the same location within a marsh. Average daily air temperatures across the month of August 2018, near our sites in FL, SC, and VA were about 27.3 °C ± 1.1 °C, 27.2 °C ± 1.1 °C, and 26.0 °C ± 2.1 °C, respectively (mean ± SD) (Weather Underground, 2018).

Snails were transported to a laboratory at the University of Georgia in Athens on August 18. During transportation, we kept snails from different sites in separate terraria covered with mesh, along with mud and stalks of *Spartina*, both alive and dead, haphazardly clipped from the collection site, to provide both natural habitat and a food source. Upon reaching Athens, we placed all 3 terraria with *Littoraria* into a Percival incubator (model I-36VL) at 27 °C with a 24-hour dark cycle and allowed them to acclimate for 48 hours. As in the respiration experiment, *Littoraria* individuals were misted with freshwater to prevent desiccation but were otherwise not submerged.

We took some of the *Spartina* we had collected from each site, rinsed it with freshwater, and dried it at 60 °C until it reached a constant mass. We then ground that *Spartina* (both stems and leaves) into a fine powder, using a ball-mill grinder, combined the ground *Spartina* powder from each site to create a homogenized powder, mixed the homogenized *Spartina* powder with agar and deionized water to form an agar solution, and then autoclaved that agar at 121 °C. We placed the resulting agar solution into a warm water bath and then decanted 10 mL of agar into petri dishes (25 mm tall and 100 mm in diameter); the agar was ~1.3 mm thick. We allowed the plates to cool within a sterile biosafety cabinet before being refrigerated until use.

Feeding experiment: experimental design

Following the initial 48 hours of acclimation in the lab, we sorted *Littoraria* into 3 size classes: large (19.43 ± 1.06 mm shell height; 84.31 ± 13.67 mg dry mass), medium (15.16 ± 1.34 mm; 44.31 ± 10.86 mg), and small (10.27 ± 1.01 mm; 16.03 ± 5.3 mg) (mean \pm SD) (Fig. A5). After *Littoraria* individuals were sorted, they were returned to an incubator at 27 °C for about 8 to 14 days, receiving new artificial seawater and fresh *Spartina* every 2 to 3 days. Because we had access to only four Percival incubators (model I-36VL) for our trials, all seven temperature treatments could not be run simultaneously. Instead, we ran concurrent trials at 25 °C, 30 °C, 40 °C, and 50 °C from August 29 to September 1 and trials at 20 °C, 35 °C, and 45 °C from September 4 to September 7. Before beginning a set of trials, we haphazardly selected 15 snails from each site (5 of each size category) for each temperature treatment and starved them for 24 hours before assigning each snail to its own petri dish. After snails were added to the petri dishes, they were allowed to feed independently (1 snail per dish) for 72 hours at the assigned temperature treatment. Petri dishes within each incubator were kept in a water bath (shallow enough not to flood the dishes) to prevent the agar from drying out. We also added three petri dishes with no snails to each incubator to control for any losses of agar not caused by snails. We placed HOBO temperature loggers (Onset Computer Corporation, Bourne, MA) adjacent to the water bath housing the agar petri dishes to ac-

count for differences across our 4 incubators; logger readings averaged across the 72-hour trial were used as the actual treatment temperature to model thermal performance. At the end of the 72-hour trial, we removed all snails from the dishes. Snails were not reused in any other trials. We then took pictures of each petri dish against a black background to aid in image analysis. This procedure resulted in 7 temperature treatments (20 °C, 25 °C, 30 °C, 35 °C, 40 °C, 45 °C, and 50 °C) for 3 size classes (small, medium, and large) from each of 3 sites (FL, SC, VA), with 5 replicates per treatment combination, resulting in a total of 315 snails (plus the 21 control dishes).

Feeding experiment: analysis

To quantify the consumption of the agar by the *Littoraria*, we used ImageJ (<https://imagej.nih.gov/ij/>) to trace the edges of the consumed area of the agar gel across the entire dish and distinguished between areas in which the agar was completely consumed (*i.e.*, the bottom of the plate was visible in these areas) from those in which the agar was only partially consumed (*i.e.*, where *Littoraria* had consumed agar gel but the plate was not fully visible). We then estimated the total amount of agar consumed as

$$\text{Total Consumption} = \text{Full} + 1/2(\text{Partial}), \quad (4)$$

where “Full” represents the area that was completely consumed and “Partial” represents the area that was partially consumed (*i.e.*, some agar was still present in the feeding area). We used this visual method rather than weighing the agar because of variability in water loss from the agar. Estimated consumption in the control dishes was always 0, so we did not make any adjustments to the feeding estimates.

We took a similar statistical approach as in the respiration experiment. We fit the modified Sharpe-Schoolfield (equation 2) and Gaussian (equation 3) models to feeding data by using a generalized non-linear least squares regression (gnls function in the nlme package ver. 3.1-152; Pinheiro *et al.*, 2021), with variances increasing with mass. We analyzed each site separately to test for mass dependency of thermal traits and then compared the best models with ones that included temperature dependence of mass scaling (α). Confidence intervals on parameters and on the TPCs were obtained as detailed in the respiration experiment.

In contrast to the respiration experiment, the feeding experiment allowed us to evaluate interpopulation variation. We therefore tested for site-dependent variation in thermal and mass-scaling parameters by using the most parsimonious model structure from our initial analyses of each site. This approach allowed us to directly evaluate the significance of site-specific parameter estimates for all combinations of parameters.

Results

Respiration experiment: mass and temperature dependencies

Although application of the Sharpe-Schoolfield model was informative, the simpler Gaussian model fit better when comparing across the most parsimonious models ($\Delta\text{AIC}_c = 3.76$ and $\Delta\text{BIC} = 6.83$; Table 1). Data best supported the Gaussian model that included mass dependency of T_{opt} (which outperformed the null model: $\Delta\text{AIC}_c = 5.23$ and $\Delta\text{BIC} = 2.11$, $P = 0.0066$; Fig. 1; Tables 2, 3), and the inclusion of mass dependency in c did not improve model fit (Table 2). Estimates of T_{opt} from the best Gaussian model (and bootstrapped confidence intervals) were 36.4 °C (34.7 to 36.4 °C), 37.6 °C (36.2 to 39.2 °C), and 40.6 °C (38.1 to 42.5 °C) for the small (8.01 mg), medium (30.87 mg), and large (86.28 mg) snails, respectively—estimates that were almost identical to those obtained with the Sharpe-Schoolfield model: 36.8 °C (33.8 to 40 °C), 37.3 °C (34.3 to 40 °C), and 40.2 °C (35.6 to 49.2 °C), respectively. Such similarity suggests that our conclusion that thermal traits are dependent on snail mass is robust to model structure. Across both models, the addition of an effect of temperature on the mass-scaling parameter (α) did not significantly improve model fit (Gaussian: $\Delta\text{AIC}_c = -1.96$ and $\Delta\text{BIC} = -5.04$, $P = 0.64$; Sharpe-Schoolfield: $\Delta\text{AIC}_c = 0.13$ and $\Delta\text{BIC} = -2.92$, $P = 0.13$; Table 1).

The Sharpe-Schoolfield model with the lowest AIC_c and BIC , while less parsimonious than the top Gaussian model, included mass dependency in E_h (temperature-induced enzymatic inactivation), a parameter that influences T_{opt} (Tables A2, A3; Fig. A1). Larger snails had lower E_h relative to smaller snails (*i.e.*, $\beta_{E_h} < 0$). This model was significantly

Table 1

Model comparisons to assess temperature dependency in mass scaling (α), using the Sharpe-Schoolfield and Gaussian models fit to the data from the respiration experiment for *Littoraria irrorata*

Model	Mass dependency	Temperature dependency	K	AIC_c	BIC
Sharpe-Schoolfield	E_h	None	8	436.24	461.51
Sharpe-Schoolfield	E_h	α	9	436.11	464.43
Gaussian	T_{opt}	None	7	432.48	454.68
Gaussian	T_{opt}	α	8	434.44	459.72

All models include the best form of mass-dependent thermal traits, either with or without the temperature dependency in α . For both the Sharpe-Schoolfield and Gaussian models, the addition of temperature dependency in α did not improve model fit. K gives the number of parameters in each model. The dataset consists of 192 estimates of respiration rates (CO_2 ppm min^{-1}). α , mass-scaling exponent; AIC_c , Akaike information criterion for small sample sizes; BIC , Bayesian information criterion; E_h , deactivation energy; T_{opt} , temperature at which a respiration rate is maximal.

better than the null model without any mass-dependent terms (mass dependency in E_h vs. null model: $\Delta\text{AIC}_c = 7.93$ and $\Delta\text{BIC} = 4.85$, $P = 0.0015$; Table A2), as was the second-best model, which included mass dependence in T_h (mass dependency in T_h vs. null model: $\Delta\text{AIC}_c = 6.35$ and $\Delta\text{BIC} = 3.27$, $P = 0.0035$; Table A2). Notably, neither of the top two best models were significantly better than the other (ΔBIC and $\Delta\text{AIC}_c = 1.58$). The only model that was indistinguishable from the null model included the mass dependency of only E_a ($\Delta\text{AIC}_c = 1.55$ and $\Delta\text{BIC} = -1.53$, $P = 0.054$; Table A2).

Thus, the metabolic rate data support the hypothesis that thermal traits (T_{opt} but not c in equation 3; E_h or T_h but not E_a in equation 2) were modified by snail mass but do not support the hypothesis that the mass scaling (α) was modified by temperature.

Feeding experiment: mass and temperature dependencies

The Gaussian and Sharpe-Schoolfield models led to similar interpretations of mass and temperature dependencies; however, the Gaussian model provided a more parsimonious fit to the data relative to the Sharpe-Schoolfield model (*i.e.*, $\Delta\text{BIC} > 2$ for each of the 3 sites; Tables 4, A4). At all three sites, the best Gaussian model lacked any mass dependency of thermal traits (Tables 4, 5). Notably, parameter estimates included rather large confidence intervals (particularly for b_{max}), suggesting that the analyses likely lack power to detect mass dependency of feeding rates. In an effort to more conservatively compare across our sites and reduce the potential for model overfitting, we chose to present results from the simpler null models for both model structures (Tables 5, A5). The addition of temperature dependence in the mass-scaling term did not improve model fit for either model (Tables 4, A4). The Gaussian model produced estimates for T_{opt} of 28.45 °C (± 3.92), 25.95 °C (± 4.52), and 31.01 °C ($\pm 2.35^\circ\text{C}$) for FL, SC, and VA, respectively (95% CI; Table 5), while the Sharpe-Schoolfield model led to similar estimates of 28.3 °C (18.7 to 30.9 °C), 25.6 °C (18.7 to 31.6 °C), and 29.7 °C (24.7 to 33.1 °C) for the 3 populations (FL, SC, and VA, respectively; 95% CI). However, raw feeding rates were relatively low and quite variable.

Interpopulation variation

The model structure that best fit the feeding data from each site separately (*i.e.*, the null Gaussian model without temperature-dependent mass scaling or mass-dependent thermal traits) provided significant support for between-population variation in feeding rates. Across all 16 models, the best model included site-specific parameters for the peak rate of feeding (b_{max}) and mass scaling (α) (Fig. 2; Table 6). This model was significantly better than a model that did not include site-specific parameters ($P < 0.0001$). Estimates of mass scaling (α) were highest for SC ($1.82^\circ\text{C} \pm 0.67^\circ\text{C}$),

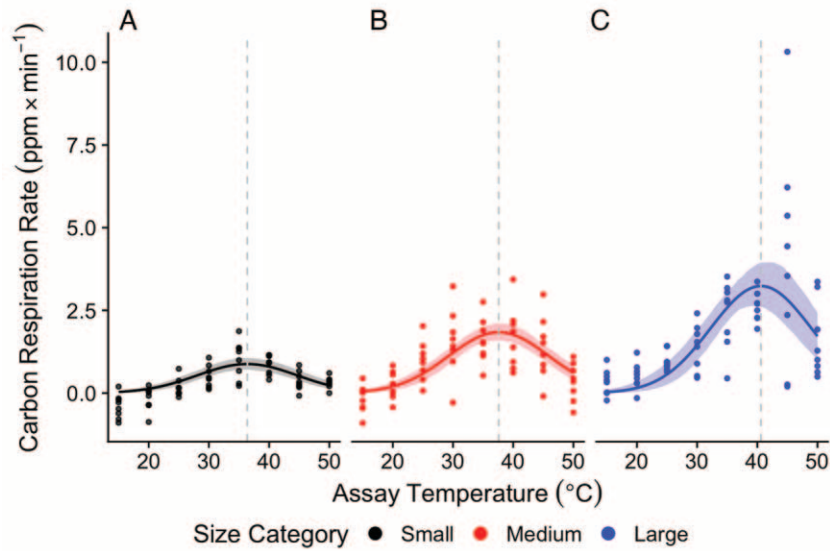


Figure 1. Thermal performance curves (TPCs) fit to data from the respiration experiment for *Littoraria irrorata*, using the best Gaussian model with effects of mass on the thermal trait E_h (deactivation energy). Blue, red, and black lines represent predicted performance for an individual of median size within the (A) large (86.28 mg), (B) medium (30.87 mg), and (C) small (8.01 mg) size classes, respectively. Points represent measurements of snail respiration rates ($\text{ppm CO}_2 \text{ min}^{-1}$) for 24 snails, each measured at all 8 temperatures. Dashed gray lines represent the temperature at peak respiration (*i.e.*, T_{opt}). Confidence intervals (95%) were bootstrapped using 500 runs.

followed by VA ($1.75 \text{ }^\circ\text{C} \pm 0.24 \text{ }^\circ\text{C}$) and FL ($1.10 \text{ }^\circ\text{C} \pm 0.18 \text{ }^\circ\text{C}$), whereas peak feeding rates follow the opposite pattern (0.0092 ± 0.0058 , 0.00069 ± 0.00067 , and 0.00021 ± 0.00059 in FL, VA, and SC, respectively). The single estimates of T_{opt} and c estimated for all sites were $29.69 \text{ }^\circ\text{C} (\pm 1.68)$ and $12.52 \text{ }^\circ\text{C} (\pm 2.17; 95\% \text{ CI})$, respectively.

Discussion

Thermal traits associated with respiration were affected by body mass. Notably, both the Gaussian and Sharpe-

Table 2

Model comparisons to assess mass dependency in thermal traits, using the Gaussian model fit to the data from the respiration experiment for *Littoraria irrorata*

Mass dependency	K	AIC_c	ΔAIC_c	BIC	ΔBIC
T_{opt}	7	432.48	0.82	454.68	0.00
None (null model)	6	437.70	6.03	456.79	2.11
T_{opt}, c	8	431.66	0.00	456.94	2.26
c	7	435.66	4.00	457.86	3.18

The best-fitting model included mass dependency of T_{opt} , with ΔAIC_c and ΔBIC calculated relative to that best model. K gives the number of parameters in the model. The dataset consists of 192 estimates of respiration rates ($\text{CO}_2 \text{ ppm min}^{-1}$). AIC_c , Akaike information criterion for small sample sizes; BIC, Bayesian information criterion; c , controls the width of the thermal performance curve; T_{opt} , temperature at which respiration rate is maximal.

Schoolfield models led to similar interpretations of mass dependencies; however, the better fit of the Gaussian model suggests that the TPC was relatively symmetric, rendering the additional complexity of the Sharpe-Schoolfield model uninformative. While the thermal traits associated with feeding rates did not exhibit mass dependency, populations from VA and SC exhibited noticeably larger effects of mass on feeding rates than did the FL population (*via* the mass-scaling parameter, α). Taken together, these results demonstrate that the application of a single TPC across sites and size classes is likely to provide misleading insights about responses of natural populations to their thermal environment. Interestingly, our study provided no support for the effect of temperature on the mass scaling (α) of either respiration or feeding rates.

Our results suggest that exploration of intraspecific variation in thermal traits warrants further consideration. Notably, mass dependencies (as we observed for respiration) and context-dependent variation in thermal traits (as documented by Gaitán-Espitia *et al.*, 2013, 2014; Luhring and DeLong, 2016; Padfield *et al.*, 2016; Tüzün *et al.*, 2017; Stager *et al.*, 2021, to name a few) will give rise to varying thermal sensitivity and thermal maxima (T_{opt}) as well as differences in the magnitudes of peak performance at these thermal maxima. As a result of this variation, population responses to temperature will vary across space (*e.g.*, latitude) and time (*e.g.*, with climate change) (Sinclair *et al.*, 2016). These differences will be exacerbated if populations have different size structures. To

Table 3

Parameter estimates (and 95% confidence intervals [CIs]) of the most parsimonious Gaussian model fit to the data from the respiration experiment for *Littoraria irrorata* ($n = 192$)

Parameter	Estimate	Lower 95% CI	Upper 95% CI
b_{max}	0.28	0.16	0.40
α	0.55	0.44	0.66
c	8.36	7.10	9.62
T'_{opt}	35.9	33.9	38.0
$\beta_{T_{opt}}$	0.054	0.016	0.092

Mass dependency of T_{opt} in the Gaussian model was modeled as a linear function of mass ($T_{opt} = T'_{opt} + \beta_{T_{opt}}M$) in which T'_{opt} (the maximum respiration rate at a mass of 0 mg) gives the estimated intercept and $\beta_{T_{opt}}$ (the linear change in T_{opt} with a 1-mg change in mass) gives the slope (*i.e.*, the effect of mass on the parameter). CI, confidence interval. α , mass-scaling exponent; b_{max} , an individual's peak rate of respiration occurring at T_{opt} ; c , controls the width of the thermal performance curve.

illustrate the effects of size structure and variation in TPC parameters on population-level feeding rate, we applied the best-fitting Gaussian model to three natural *Littoraria* populations that differed in size structure but had relatively similar densities (Fig. 3A). Even in the absence of mass-dependent thermal traits, and when evaluated using the same thermal parameters, these populations (because of their different size structures) varied considerably in predicted feeding rates (Fig. 3B, C).

When we applied the three different sets of parameters to these three size structures, even more striking differences emerged. For example, when the size structure was skewed toward large individuals (Fig. 3B), the parameters from VA led to higher population-level feeding at most temperatures (compared to the parameters from FL and SC): the expected feeding rate using the VA parameters was about twice as great as the feeding rate using SC parameters. Even more important, these patterns were affected by size structure. For example, in the population comprised predominately of smaller individuals, the expected feeding rate using the FL parameters was two to five times greater than the feeding rates using the VA or SC parameters (Fig. 3D). Thus, between-site variation in TPC parameters influenced the magnitude of differences in peak performance, and the nature of this effect depended on the size structure of the population (Fig. 3).

The temperature at which respiration rate was maximal (T_{opt}) increased with body size (Fig. 1), an intraspecific pattern that has rarely been explored (but see Kingsolver *et al.*, 2011; Rebolledo *et al.*, 2020). Interestingly, we did not see this same pattern with feeding rate (Fig. 2), where mass dependency of thermal traits was not detected. Across aquatic species, Leiva *et al.* (2019) noted that resistance to long-term heat and cold is enhanced in smaller- and larger-bodied species, respectively, likely owing to a combination of oxygen diffusion efficiency at warmer temperatures and the abil-

ity to use energetic reserves to withstand colder temperatures. In contrast, two species of soil arthropod exhibited a significant negative relationship between body size and critical thermal maximum, whereas one juvenile stage of spider exhibited a positive relationship (Franken *et al.*, 2018). Within *Littoraria*, a positive relationship between body size and T_{opt} for respiration suggests that larger individuals are able to tolerate slightly hotter acute temperature exposure before beginning to experience physiological suppression. Furthermore, T_{opt} extracted from the best Sharpe-Schoolfield model for respiration was primarily driven by the mass dependency of the declining part of the curve (E_h) associated with high-temperature inactivation of metabolism (Fig. A6, top left panel); that is, large individuals had less of a decline in respiration than expected under the model with no mass dependencies, and smaller individuals had a greater than expected decline. The value for T_{opt} fit by the more parsimonious Gaussian model (*i.e.*, with an interaction between T_{opt} and body mass), while also shifted right for large individuals, exhibited a higher maximum respiration rate than expected

Table 4

Model comparisons to assess mass dependency in thermal traits, using the Gaussian model fit to the data from the feeding experiment for *Littoraria irrorata*

Mass dependency	Temperature dependency	K	AIC _c	Δ AIC _c	BIC	Δ BIC
Florida						
None (null model)	None	6	17.29	0.00	32.36	0.00
None	α	7	18.76	1.47	36.19	3.82
c	None	7	19.31	2.01	36.73	4.37
T_{opt}	None	7	19.48	2.19	36.90	4.54
T_{opt}, c	None	8	21.65	4.36	41.38	9.02
South Carolina						
None (null model)	None	6	-148.68	0.00	-133.62	0.00
None	α	7	-148.61	0.07	-131.19	2.43
T_{opt}	None	7	-147.27	1.41	-129.85	3.77
c	None	7	-147.16	1.52	-129.74	3.88
T_{opt}, c	None	8	-146.32	2.37	-126.58	7.03
Virginia						
None (null model)	None	6	39.15	0.52	54.22	0.00
c	None	7	38.63	0.00	56.06	1.84
T_{opt}	None	7	41.39	2.76	58.81	4.60
None	α	7	41.45	2.81	58.87	4.65
T_{opt}, c	None	8	40.64	2.01	60.37	6.15

Data from each of the three sites were fit separately ($n = 105$ snails per site). The best-fitting model for all three sites was the null model, which lacked mass dependency; Δ AIC_c and Δ BIC are calculated relative to that best model. K gives the number of parameters in each model. α , mass-scaling exponent; AIC_c, Akaike information criterion for small sample sizes; BIC, Bayesian information criterion; c , controls the width of the thermal performance curve; T_{opt} , temperature at which feeding rate is maximal.

Table 5

Parameter estimates (and 95% confidence intervals [CIs]) from the most parsimonious (lowest Bayesian information criterion) Gaussian model fit to the data from the feeding experiment for *Littoraria irrorata*

Parameter	Site	Estimate	Lower 95% CI	Upper 95% CI
b_{max}	FL	0.00843	0.00121	0.0157
	SC	0.000265	-0.0000692	0.00060
	VA	0.000755	-0.00000618	0.00152
α	FL	1.12	0.90	1.35
	SC	1.78	1.46	2.10
	VA	1.73	1.48	1.98
T_{opt}	FL	28.5	24.5	32.4
	SC	26.0	21.4	30.5
	VA	31.0	28.7	33.3
c	FL	13.7	8.8	18.7
	SC	12.9	7.8	18.0
	VA	11.8	8.8	14.8

The model does not include any effect of mass on the thermal traits or temperature on mass scaling and was applied separately to each of the three study populations (Florida [FL], South Carolina [SC], and Virginia [VA]). $n = 105$ snails per site. α , mass-scaling exponent; b_{max} , an individual's peak rate of feeding occurring at T_{opt} ; c , controls the width of the thermal performance curve; T_{opt} , temperature at which feeding rate is maximal.

under both the null Gaussian model (with no mass dependencies) and the Sharpe-Schoolfield model (Fig. A6, bottom left panel). Such findings warrant further exploration of how larger individuals may enhance their performance at high temperatures and whether this is a beneficial response, partic-

ularly given that a lack of mass dependency of feeding rate suggests that larger snails may be less able to compensate for their greater energetic expenditure at increased temperatures. It is worth noting that, in larger individuals, intraspecific variation in respiration at high temperatures is quite large (see data in Fig. 1 for large individuals at 45 °C). The two highest temperatures used in our experiments were near the upper thermal limit for *Littoraria* (Bingham, 1972; Iacarella and Helmuth, 2011); and the variability in respiration rates around such temperatures could indicate that some individuals experienced extreme stress, including heat coma (Shirley *et al.*, 1978; Iacarella and Helmuth, 2011) or even death (during which continued metabolic reactions are still possible: DeLong *et al.*, 2017). Sandison (1967) observed that the aerial respiration rates of intertidal snails increased sharply at the onset of heat coma, before falling near the lethal thermal limit. This could explain why such variability in thermal response was not apparent at 50 °C (*i.e.*, past the onset of heat coma) but cannot explain the lack of a similar pattern in respiration rates in either of the smaller size classes. Last, while the effects of heat coma are reversible, we did not monitor the recovery of individual *Littoraria* after the respiration experiment and thus cannot evaluate these hypotheses.

Given the observed variation between populations in their TPCs, it will be important to disentangle the extent to which differences in thermal traits across populations are due to genetic differentiation *versus* plasticity. Planktonic larval dispersion of *Littoraria* across populations is not well understood, but one study reports insignificant genetic differentiation across the marshes that span our study sites (Díaz-Ferguson *et al.*,

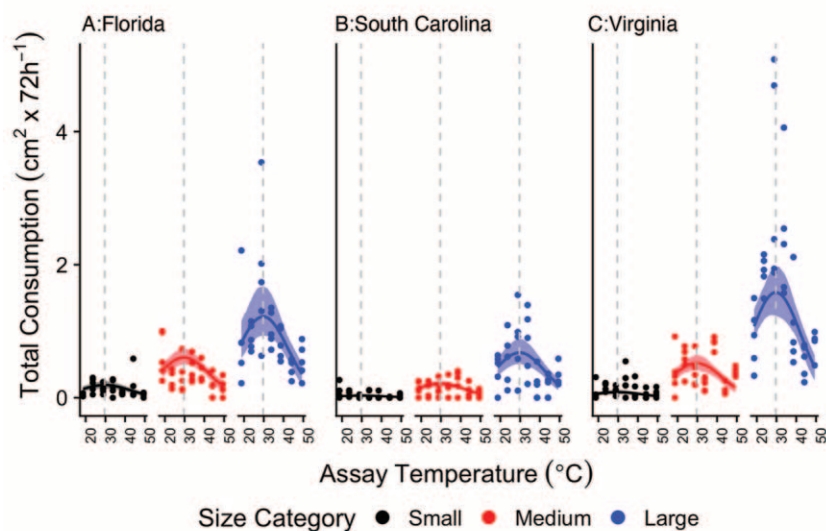


Figure 2. Thermal performance curve (TPCs) fit to data from the feeding experiment for *Littoraria irrorata*, using the Gaussian model without effects of mass on thermal traits. Blue, red, and black lines represent predicted performance for an individual of median size within the large (83.24 mg), medium (44.03 mg), and small (15.48 mg) size classes, respectively. Points represent measurements of snail feeding rates (cm^2 *Spartina* agar) over 72 hours across sites in (A) Florida, (B) South Carolina, and (C) Virginia ($n = 105$ snails per site) for a total of 315 snails. Confidence intervals (95%) were bootstrapped using 500 runs.

Table 6

Model comparisons to assess site interactions in thermal traits, using the Gaussian model fit to the data from the feeding experiment for *Littoraria irrorata*

Site-specific parameters	K	AIC _c	ΔAIC _c	BIC	ΔBIC
b_{max}, α	10	-25.22	0.00	11.58	0.00
b_{max}	8	-11.56	13.66	17.99	6.40
T_{opt}, b_{max}, α	12	-23.80	1.42	20.20	8.61
α	8	-8.48	16.74	21.07	9.49
b_{max}, c, α	12	-21.45	3.77	22.55	10.97
T_{opt}, b_{max}	10	-9.99	15.23	26.81	15.23
b_{max}, c	10	-7.41	17.81	29.40	17.81
T_{opt}, α	10	-6.86	18.36	29.94	18.36
$T_{opt}, b_{max}, c, \alpha$	14	-20.69	4.53	30.45	18.87
c, α	10	-4.72	20.50	32.08	20.50
T_{opt}	8	4.30	29.51	33.85	22.26
T_{opt}, b_{max}, c	12	-6.05	19.17	37.95	26.36
T_{opt}, c, α	12	-4.70	20.52	39.30	27.72
c	8	16.44	41.65	45.99	34.40
T_{opt}, c	10	17.14	42.36	53.94	42.36
None (null model)	6	51.82	77.04	74.06	62.48

Data from each of the three sites were fit collectively ($n = 315$ snails). The best-fitting model for all three sites was the model with site-specific coefficients for b_{max} and α ; ΔAIC_c and ΔBIC are calculated relative to that best model. K gives the number of parameters in each model. α , mass-scaling exponent; AIC_c, Akaike information criterion for small sample sizes; BIC, Bayesian information criterion; b_{max} , an individual's peak rate of feeding occurring at T_{opt} ; c , controls the width of the thermal performance curve; T_{opt} , temperature at which feeding rate is maximal.

2010). Thus, it seems unlikely that these differences in feeding and respiration have a genetic basis. Instead, the intraspecific variation we documented may reflect incomplete acclimation if snails experienced very different thermal environments prior to collection. However, average daily air temperatures across each site were within 1.5 °C of each other at the time of collection (Weather Underground, 2018). In contrast, the monthly temperature range (max–min) at these 3 sites is positively related to latitude, spanning ~14 °C to 19 °C. Furthermore, while our study was conducted during the summer months, when average air temperatures were similar across sites, this does not preclude seasonal differences from driving differentiation in acclimation abilities (Rohr *et al.*, 2018); for example, while average monthly water temperature in the summer is independent of latitude between sites spanning about 5 degrees of latitude (the latitudinal difference between our sites), this relationship becomes significantly negative in the spring, winter, and fall (Byers *et al.*, 2015). Our total temperature acclimation times across experiments (~2–9 days for the respiration experiment and ~10–16 days for the feeding experiment) are in line with previous work measuring littorinid gastropod physiology (*e.g.*, Henry *et al.*, 1993). McMahon *et al.* (1995) found no metabolic acclimation to temperature in the respiration rate of two species of intertidal littorinids in

the summertime (acclimated for 15–20 days at 4 °C or 21 °C). However, in *Littoraria irrorata*, snails acclimated during the winter season to a cold temperature treatment (0 °C) for 5 days consumed significantly less oxygen at 6 °C than snails acclimated to a hot temperature treatment (23 °C), a behavior that was indicative of *Littoraria* entering hibernation (Paul *et al.*, 1989). If our results were driven by seasonal differences in experienced temperatures, it suggests that acclimation is a very long-term process.

One final caveat worth noting in the feeding experiment is that we kept individuals in total darkness, which may have dampened the circadian rhythm of oxygen consumption and, thus, possibly feeding activity (Shirley and Findley, 1978). Furthermore, values of α in our feeding study were relatively large (1.1–1.8) compared to mass-scaling values in the literature for both respiration and consumption rates, which typically range from 0.4 to 1.2 and from 0.6 to 1.1,

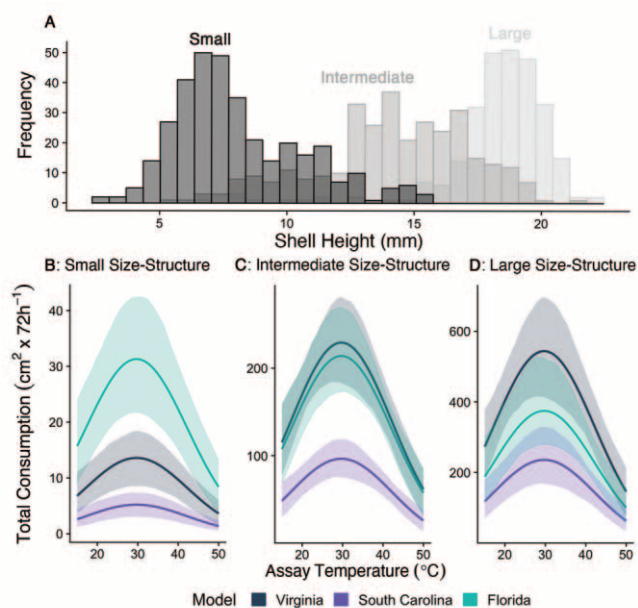


Figure 3. Exploring population-level feeding as a function of population-specific feeding parameters and size structures. (A) Size structure of *Littoraria irrorata* from three sites that exhibit different size structure but similar densities. Small (dark gray) is from Sapelo Island, Georgia, with a density of 347 snails per 8000 cm² (total number in 5 40 cm × 40 cm² quadrats); medium (midgray) is from Fort Fisher State Recreation Area, North Carolina, with a density of 318 snails per 8000 cm²; and large (light gray) is from Goodwin Island, Virginia, with a density of 273 snails per 8000 cm². Predicted population-level thermal performance curves (TPCs) for feeding based on the best-fitting Gaussian model (without mass or temperature dependencies but with site-specific estimates of T_{opt} [temperature at which feeding rate is maximal], b_{max} [an individual's peak rate of feeding occurring at T_{opt}], c [controls the width of the thermal performance curve], and α [mass-scaling exponent]) for populations from Virginia, South Carolina, and Florida and applied to the size structure of three populations that span a range of size distributions: (B) small, (C) intermediate, and (D) large size structures. Confidence intervals (95%) were bootstrapped using 500 runs and were based on uncertainty in the TPC parameters (not the size structure).

respectively (see fig. 1 in Glazier, 2005 and fig. 3b for marine invertebrates in Rall *et al.*, 2012). Pawar *et al.* (2012) showed that scaling relationships for feeding rate tend to be steeper (~ 1) when resources are abundant, a common condition in laboratory experiments. Our large values of α might also have arisen from photographic methods in the feeding experiment; if feeding of smaller individuals was less likely to be detected in the photographs relative to that of larger individuals, we may have biased our estimation of α to larger values. Finally, given the differences in experimental contexts, and in the season during which our respiration and feeding experiments were conducted, we caution against directly comparing parameter estimates from these two studies (Shirley *et al.*, 1978), for example, to estimate scope for growth (Strong and Daborn, 1980; Hoefnagel and Verberk, 2017). However, it remains notable that the T_{opt} from these two experiments differed by ~ 10 °C, even across snails collected at the same site (FL).

In general, there remains a disconnect between broad, multitaxa syntheses and small-scale, single-species studies of ecophysiology. This gap might reflect our limited understanding of how thermal traits at higher levels of organization (*e.g.*, populations) are shaped by processes occurring at lower levels of organization (*e.g.*, molecules and cellular environments). For example, the upward slope of TPCs for protein function, as indicated by E_a , while variable, does not exhibit a clear relationship with habitat or taxa (Schulte, 2015). Meanwhile, E_a varies appreciably across taxa, increasing in magnitude and variability with the level of organization (*i.e.*, interspecific variation in E_a is relatively small for chemical functionality and much greater at the whole-population level; Dell *et al.*, 2011). Future research should aim to understand how variation in thermal performance at one level (*e.g.*, molecular) translates into variation in performance at higher levels of organization (*e.g.*, between individuals and across populations) (see Rezende and Bozinovic, 2019; Bozinovic *et al.*, 2020).

Although our study provides evidence for intraspecific mass interactions with, and cross-site variation in, thermal traits, and points to the need to further consider these sources of intraspecific variation, there are limitations to how thermal performance curves generated in a lab setting can be applied to natural populations. Consideration should be given to the relative importance of temperature ramping rate, exposure time, and fluctuations in how they affect physiological responses and thermal performance traits (Chown *et al.*, 2009; Clusella-Trullas *et al.*, 2011; Magozzi and Calosi, 2015; Kingsolver and Woods, 2016; Cavalheri *et al.*, 2019; Cloyed *et al.*, 2019; Domínguez-Guerrero *et al.*, 2020). As new studies are performed, we also look forward to the development of conceptual frameworks that link intraspecific variation in performance metrics to their underlying physiological mechanisms, environmental drivers, and population- and community-level implications.

Acknowledgments

We thank the Guana Tolomato Matanzas National Estuarine Research Reserve (GTM-NERR), the North Inlet Winyah Bay National Estuarine Research Reserve (NIWB-NERR), the Sapelo Island National Estuarine Research Reserve (SI-NERR), the Nature Conservancy of Virginia Preserves, and the University of Georgia Marine Institute (and Georgia Coastal Ecosystems Long Term Ecological Research [GCE LTER]) for facilitating access to field sites. This work was funded by a National Science Foundation Graduate Research Fellowship Program and an M.K. Pentecost Ecology Fund grant to RLA and through several assistantships awarded through the Center for Undergraduate Research Opportunities (CURO) at the University of Georgia. We would also like to thank Drs. Ford Ballantyne, Jeb Byers, and John Drake for the use of lab facilities. Finally, we thank members of the Osenberg lab (especially Elizabeth Hamman and Phil Shirk) and Claire Teitelbaum for their continued guidance and insight on experimental design, analysis, and interpretation.

Ethical Care Consideration

All experiments were conducted in an ethical manner. Permits and approvals were obtained for use of field sites (Guana Tolomato Matanzas National Estuarine Research Reserve [GTM-NERR], NIWB-NERR [North Inlet Winyah Bay National Estuarine Research Reserve], and the Nature Conservancy in Virginia [VA-TNC]) and the scientific collection of *Littoraria* (Florida Fish and Wildlife Conservation Commission Special Activity License [FWC SAL] license SAL-17-1936-SR; Virginia Department of Game and Inland Fisheries [VADGIF] permit 065073). All *Littoraria* individuals were maintained at a laboratory at the University of Georgia in Athens. At the conclusion of each experiment, all *Littoraria* specimens were frozen and will be donated to the University of Georgia Museum of Natural History after the publication of this work.

Data Accessibility

Data and code will be made available within the Georgia Coastal Ecosystem (GCE) Long-Term Ecological Research (LTER) program's online data catalog (https://gce-lter.marsci.uga.edu/public/app/data_catalog.asp).

Literature Cited

- Angilletta, M. J. 2006. Estimating and comparing thermal performance curves. *J. Therm. Biol.* **31**: 541–545.
- Angilletta, M. J., R. B. Huey, and M. R. Frazier. 2010. Thermodynamic effects on organismal performance: Is hotter better? *Physiol. Biochem. Zool.* **83**: 197–206.
- Atkins, R. L., J. N. Griffin, C. Angelini, M. I. O'Connor, and B. R. Siliman. 2015. Consumer-plant interaction strength: importance of body size, density and metabolic biomass. *Oikos* **124**: 1274–1281.

- Bartoń, K. 2020.** MuMIn: multi-model inference. R package version 1.43.17. [Online]. Available: <https://CRAN.R-project.org/package=MuMIn> [2022, May 3].
- Bates, D., M. Maechler, B. Bolker, and S. Walker. 2015.** Fitting linear mixed-effects models using lme4. *J. Stat. Softw.* **67**: 1–48.
- Bingham, F. O. 1972.** The influence of environmental stimuli on the direction of movement of the supralittoral gastropod *Littorina irrorata*. *Bull. Mar. Sci.* **22**: 309–335.
- Bistransin, M. E. 1976.** The reproductive physiology of the prosobranch snail *Littorina irrorata* (Say, 1822). MS thesis, Louisiana State University, Baton Rouge.
- Bozinovic, F., G. Cavieres, S. I. Martel, J. M. Alruiz, A. N. Molina, H. Roschztardt, and E. L. Rezende. 2020.** Thermal effects vary predictably across levels of organization: empirical results and theoretical basis. *Proc. R. Soc. B Biol. Sci.* **287**: 20202508.
- Brown, J. H., J. F. Gillooly, A. P. Allen, V. M. Savage, and G. B. West. 2004.** Toward a metabolic theory of ecology. *Ecology* **85**: 1771–1789.
- Byers, J. E., J. H. Grabowski, M. F. Piehler, A. R. Hughes, H. W. Weiskel, J. C. Malek, and D. L. Kimbro. 2015.** Geographic variation in intertidal oyster reef properties and the influence of tidal prism: biogeography of intertidal oyster reefs. *Limnol. Oceanogr.* **60**: 1051–1063.
- Carey, N., and J. D. Sigwart. 2014.** Size matters: Plasticity in metabolic scaling shows body-size may modulate responses to climate change. *Biol. Lett.* **10**: 20140408.
- Cavalheri, H. B., C. C. Symons, M. Schulhof, N. T. Jones, and J. B. Shurin. 2019.** Rapid evolution of thermal plasticity in mountain lake *Daphnia* populations. *Oikos* **128**: 692–700.
- Chown, S. L., K. R. Jumbam, J. G. Sørensen, and J. S. Terblanche. 2009.** Phenotypic variance, plasticity and heritability estimates of critical thermal limits depend on methodological context. *Funct. Ecol.* **23**: 133–140.
- Clarke, A. 1993.** Seasonal acclimatization and latitudinal compensation in metabolism: Do they exist? *Funct. Ecol.* **7**: 139–149.
- Cloyed, C. S., A. I. Dell, T. Hayes, R. L. Kordas, and E. J. O’Gorman. 2019.** Long-term exposure to higher temperature increases the thermal sensitivity of grazer metabolism and movement. *J. Anim. Ecol.* **88**: 833–844.
- Clusella-Trullas, S., T. M. Blackburn, and S. L. Chown. 2011.** Climatic predictors of temperature performance curve parameters in ectotherms imply complex responses to climate change. *Am. Nat.* **177**: 738–751.
- Cottin, D., N. Foucreau, F. Hervant, and C. Piscart. 2015.** Differential regulation of *hsp70* genes in the freshwater key species *Gammarus pulex* (Crustacea, Amphipoda) exposed to thermal stress: effects of latitude and ontogeny. *J. Comp. Physiol. B Biochem. Syst. Environ. Physiol.* **185**: 303–313.
- Dell, A. I., S. Pawar, and V. M. Savage. 2011.** Systematic variation in the temperature dependence of physiological and ecological traits. *Proc. Natl. Acad. Sci. U.S.A.* **108**: 10591–10596.
- Dell, A. I., S. Pawar, and V. M. Savage. 2014.** Temperature dependence of trophic interactions are driven by asymmetry of species responses and foraging strategy. *J. Anim. Ecol.* **83**: 70–84.
- DeLong, J. P., J. P. Gibert, T. M. Luhring, G. Bachman, B. Reed, A. Neyer, and K. L. Montooth. 2017.** The combined effects of reactant kinetics and enzyme stability explain the temperature dependence of metabolic rates. *Ecol. Evol.* **7**: 3940–3950.
- DeLong, J. P., G. Bachman, J. P. Gibert, T. M. Luhring, K. L. Montooth, A. Neyer, and B. Reed. 2018.** Habitat, latitude and body mass influence the temperature dependence of metabolic rate. *Biol. Lett.* **14**: 20180442.
- Díaz-Ferguson, E., J. D. Robinson, B. Silliman, and J. P. Wares. 2010.** Comparative phylogeography of North American Atlantic salt marsh communities. *Estuar. Coasts* **33**: 828–839.
- Domínguez-Guerrero, S. F., B. L. Bodensteiner, A. Pardo-Ramírez, D. R. Aguillón-Gutiérrez, F. R. M. la Cruz, and M. M. Muñoz. 2020.** Thermal physiology responds to interannual temperature shifts in a montane horned lizard, *Phrynosoma orbiculare*. *J. Exp. Zool. A Ecol. Integr. Physiol.* **335**: 136–145.
- Dunham, A. E., B. W. Grant, and K. L. Overall. 1989.** Interfaces between biophysical and physiological ecology and the population ecology of terrestrial vertebrate ectotherms. *Physiol. Zool.* **62**: 335–355.
- Franken, O., M. Huizinga, J. Ellers, and M. P. Berg. 2018.** Heated communities: large inter- and intraspecific variation in heat tolerance across trophic levels of a soil arthropod community. *Oecologia* **186**: 311–322.
- Gaitán-Espitia, J. D., M. Belén Arias, M. A. Lardies, and R. F. Nespolo. 2013.** Variation in thermal sensitivity and thermal tolerances in an invasive species across a climatic gradient: lessons from the land snail *Cornu aspersum*. *PLoS One* **8**: e70662.
- Gaitán-Espitia, J. D., L. D. Bacigalupe, T. Opitz, N. A. Lagos, T. Timmermann, and M. A. Lardies. 2014.** Geographic variation in thermal physiological performance of the intertidal crab *Petrolisthes violaceus* along a latitudinal gradient. *J. Exp. Biol.* **217**: 4379–4386.
- Garzke, J., S. J. Connor, U. Sommer, and M. I. O’Connor. 2019.** Trophic interactions modify the temperature dependence of community biomass and ecosystem function. *PLoS Biol.* **17**: e2006806.
- Gillooly, J. F., J. H. Brown, G. B. West, V. M. Savage, and E. L. Charnov. 2001.** Effects of size and temperature on metabolic rate. *Science* **293**: 2248–2251.
- Glazier, D. S. 2005.** Beyond the “3/4-power law”: variation in the intra- and interspecific scaling of metabolic rate in animals. *Biol. Rev.* **80**: 611.
- Glazier, D. S. 2010.** A unifying explanation for diverse metabolic scaling in animals and plants. *Biol. Rev.* **85**: 111–138.
- Gunderson, A. R., and J. H. Stillman. 2015.** Plasticity in thermal tolerance has limited potential to buffer ectotherms from global warming. *Proc. R. Soc. B Biol. Sci.* **282**: 20150401.
- Hamilton, P. V. 1977.** Daily movements and visual location of plant stems by *Littorina irrorata* (Mollusca: Gastropoda). *Mar. Freshw. Behav. Physiol.* **4**: 293–304.
- Henry, R. P., C. J. McBride, and A. H. Williams. 1993.** Responses of the marsh periwinkle, *Littoraria (Littorina) irrorata* to temperature, salinity and desiccation, and the potential physiological relationship to climbing behavior. *Mar. Freshw. Behav. Physiol.* **24**: 45–54.
- Hobbs, J. K., W. Jiao, A. D. Easter, E. J. Parker, L. A. Schipper, and V. L. Arcus. 2013.** Change in heat capacity for enzyme catalysis determines temperature dependence of enzyme catalyzed rates. *ACS Chem. Biol.* **8**: 2388–2393.
- Hoefnagel, K. N., and W. C. E. P. Verberk. 2017.** Long-term and acute effects of temperature and oxygen on metabolism, food intake, growth and heat tolerance in a freshwater gastropod. *J. Therm. Biol.* **68**: 27–38.
- Iacarella, J. C., and B. Helmuth. 2011.** Experiencing the salt marsh environment through the foot of *Littoraria irrorata*: behavioral responses to thermal and desiccation stresses. *J. Exp. Mar. Biol. Ecol.* **409**: 143–153.
- Johnson, D. J., and Z. R. Stahlschmidt. 2020.** City limits: Heat tolerance is influenced by body size and hydration state in an urban ant community. *Ecol. Evol.* **10**: 4944–4955.
- Kingsolver, J. G., and R. B. Huey. 2008.** Size, temperature, and fitness: three rules. *Ecol. Evol. Res.* **10**: 251–268.
- Kingsolver, J. G., and H. A. Woods. 2016.** Beyond thermal performance curves: modeling time-dependent effects of thermal stress on ectotherm growth rates. *Am. Nat.* **187**: 283–294.
- Kingsolver, J. G., H. Arthur Woods, L. B. Buckley, K. A. Potter, H. J. MacLean, and J. K. Higgins. 2011.** Complex life cycles and the responses of insects to climate change. *Integr. Comp. Biol.* **51**: 719–732.
- Klockmann, M., F. Günter, and K. Fischer. 2017.** Heat resistance throughout ontogeny: Body size constrains thermal tolerance. *Glob. Change Biol.* **23**: 686–696.
- Leiva, F. P., P. Calosi, and W. C. E. P. Verberk. 2019.** Scaling of thermal tolerance with body mass and genome size in ectotherms: a comparison

- between water- and air-breathers. *Philos. Trans. R. Soc. B Biol. Sci.* **374**: 20190035. 20190035.
- Lindmark, M., M. Huss, J. Ohlberger, and A. Gårdmark. 2018.** Temperature-dependent body size effects determine population responses to climate warming. *Ecol. Lett.* **21**: 181–189.
- Luhring, T. M., and J. P. DeLong. 2016.** Predation changes the shape of thermal performance curves for population growth rate. *Curr. Zool.* **62**: 501–505.
- Lynch, M., and W. Gabriel. 1987.** Environmental tolerance. *Am. Nat.* **129**: 283–303.
- Magozzi, S., and P. Calosi. 2015.** Integrating metabolic performance, thermal tolerance, and plasticity enables for more accurate predictions on species vulnerability to acute and chronic effects of global warming. *Glob. Change Biol.* **21**: 181–194.
- McMahon, R. F., W. Russell-Hunter, and D. W. Aldridge. 1995.** Lack of metabolic temperature compensation in the intertidal gastropods, *Littorina saxatilis* (Olivi) and *L. obtusata* (L.). *Hydrobiologia* **309**: 89–100.
- Miguez, F. 2021.** nlraa: nonlinear regression for agricultural applications. R package version 0.98. [Online]. Available: <https://CRAN.R-project.org/package=nlraa> [2022, April 29].
- Miller, L. P., and M. W. Denny. 2011.** Importance of behavior and morphological traits for controlling body temperature in littorinid snails. *Biol. Bull.* **220**: 209–223.
- Monaco, C. J., E. M. D. Porporato, J. A. Lathlean, M. Tagliarolo, G. Sarà, and C. D. McQuaid. 2019.** Predicting the performance of cosmopolitan species: Dynamic energy budget model skill drops across large spatial scales. *Mar. Biol.* **166**: 14.
- Newell, R. C. 1973.** Factors affecting the respiration of intertidal invertebrates. *Am. Zool.* **13**: 513–528.
- Ohlberger, J., T. Mehner, G. Staaks, and F. Hölker. 2012.** Intraspecific temperature dependence of the scaling of metabolic rate with body mass in fishes and its ecological implications. *Oikos* **121**: 245–251.
- Padfield, D., G. Yvon-Durocher, A. Buckling, S. Jennings, and G. Yvon-Durocher. 2016.** Rapid evolution of metabolic traits explains thermal adaptation in phytoplankton. *Ecol. Lett.* **19**: 133–142.
- Paul, R. W., W. I. Hatch, J. P. Wesley, and M. J. Stein. 1989.** Behavior and respiration of the salt marsh periwinkle, *Littorina irrorata* (Say), during winter. *Mar. Behav. Physiol.* **15**: 229–241.
- Pawar, S., A. I. Dell, and V. M. Savage. 2012.** Dimensionality of consumer search space drives trophic interaction strengths. *Nature* **486**: 485–489.
- Pennings, S. C., and B. R. Silliman. 2005.** Linking biogeography and community ecology: latitudinal variation in plant-herbivore interaction strength. *Ecology* **86**: 2310–2319.
- Pennings, S. C., S. Zengel, J. Oehrig, M. Alber, T. D. Bishop, D. R. Deis, D. Devlin, A. R. Hughes, J. J. Hutchens, W. M. Kiehn et al. 2016.** Marine ecoregion and Deepwater Horizon oil spill affect recruitment and population structure of a salt marsh snail. *Ecosphere* **7**: e01588.
- Pinheiro, J., D. Bates, S. DebRoy, D. Sarkar, and R Core Team. 2021.** nlme: linear and nonlinear mixed effects models. R package version 3.1-152. [Online]. R Foundation for Statistical Computing, Vienna. Available: <https://CRAN.R-project.org/package=nlme> [2021, April 1].
- R Core Team. 2021.** R: a language and environment for statistical computing. [Online]. R Foundation for Statistical Computing, Vienna. Available: <https://www.R-project.org> [2022, April 29].
- RStudio Team. 2020.** RStudio: integrated development for R. [Online]. RStudio, PBC, Boston. Available: <http://www.rstudio.com> [2020, May 22].
- Rall, B. C., U. Brose, M. Hartvig, G. Kalinkat, F. Schwarzmüller, O. Vucic-Pestic, and O. L. Petchey. 2012.** Universal temperature and body-mass scaling of feeding rates. *Philos. Trans. R. Soc. B Biol. Sci.* **367**: 2923–2934.
- Rebolledo, A. P., C. M. Sgrò, and K. Monro. 2020.** Thermal performance curves reveal shifts in optima, limits and breadth in early life. *J. Exp. Biol.* **223**: jeb233254.
- Rezende, E. L., and F. Bozinovic. 2019.** Thermal performance across levels of biological organization. *Philos. Trans. R. Soc. B Biol. Sci.* **374**: 20180549.
- Rietl, A. J., M. G. Sorrentino, and B. J. Roberts. 2018.** Spatial distribution and morphological responses to predation in the salt marsh periwinkle. *Ecosphere* **9**: e02316.
- Rohr, J. R., D. J. Civitello, J. M. Cohen, E. A. Roznik, B. Sinervo, and A. I. Dell. 2018.** The complex drivers of thermal acclimation and breadth in ectotherms. *Ecol. Lett.* **21**: 1425–1439.
- Rubalcaba, J. G., W. C. E. P. Verberk, A. J. Hendriks, B. Saris, and H. A. Woods. 2020.** Oxygen limitation may affect the temperature and size dependence of metabolism in aquatic ectotherms. *Proc. Natl. Acad. Sci. U.S.A.* **117**: 31963–31968.
- Sandison, E. E. 1967.** Respiratory response to temperature and temperature tolerance of some intertidal gastropods. *J. Exp. Mar. Biol. Ecol.* **1**: 271–281.
- Schaum, C. E., Student Research Team, R. French-Constant, C. Lowe, J. S. Ólafsson, D. Padfield, and G. Yvon-Durocher. 2018.** Temperature-driven selection on metabolic traits increases the strength of an algal-grazer interaction in naturally warmed streams. *Glob. Change Biol.* **24**: 1793–1803.
- Schoolfield, R. M., P. J. H. Sharpe, and C. E. Magnuson. 1981.** Non-linear regression of biological temperature-dependent rate models based on absolute reaction-rate theory. *J. Theor. Biol.* **88**: 719–731.
- Schulte, P. M. 2015.** The effects of temperature on aerobic metabolism: towards a mechanistic understanding of the responses of ectotherms to a changing environment. *J. Exp. Biol.* **218**: 1856–1866.
- Sharpe, P. J., and D. W. DeMichele. 1977.** Reaction kinetics of poikilotherm development. *J. Theor. Biol.* **64**: 649–670.
- Shirley, T. C., and A. M. Findley. 1978.** Circadian rhythm of oxygen consumption in the marsh periwinkle, *Littorina irrorata* (Say, 1822). *Comp. Biochem. Physiol. A Physiol.* **59**: 339–342.
- Shirley, T. C., G. J. Denoux, and W. B. Stickle. 1978.** Seasonal respiration in the marsh periwinkle, *Littorina irrorata*. *Biol. Bull.* **154**: 322–334.
- Silliman, B. R. 2005.** Drought, snails, and large-scale die-off of southern U.S. salt marshes. *Science* **310**: 1803–1806.
- Silliman, B. R., and J. C. Ziemann. 2001.** Top-down control of *Spartina alterniflora* production by periwinkle grazing in a Virginia salt marsh. *Ecology* **82**: 2830–2845.
- Sinclair, B. J., K. E. Marshall, M. A. Sewell, D. L. Levesque, C. S. Willett, S. Slotsbo, Y. Dong, C. D. G. Harley, D. J. Marshall, B. S. Helmuth et al. 2016.** Can we predict ectotherm responses to climate change using thermal performance curves and body temperatures? *Ecol. Lett.* **19**: 1372–1385.
- Stager, M., N. R. Senner, D. L. Swanson, M. D. Carling, D. K. Eddy, T. J. Greives, and Z. A. Cheviron. 2021.** Temperature heterogeneity correlates with intraspecific variation in physiological flexibility in a small endotherm. *Nat. Commun.* **12**: 4401.
- Stagg, C. L., and I. A. Mendelssohn. 2012.** *Littoraria irrorata* growth and survival in a sediment-restored salt marsh. *Wetlands* **32**: 643–652.
- Stanhope, H., W. Banta, and M. Temkin. 1982.** Size-specific emergence of the marsh snail, *Littorina irrorata*: effect of predation by blue crabs in a Virginia salt marsh. *Gulf Caribb. Res.* **7**: 179–182.
- Stiven, A. E., and J. T. Hunter. 1976.** Growth and mortality of *Littorina irrorata* Say in three North Carolina marshes. *Chesapeake Sci.* **17**: 168–176.
- Strong, K. W., and G. R. Daborn. 1980.** The influence of temperature on energy budget variables, body size, and seasonal occurrence of the isopod *Idotea baltica* (Pallas). *Can. J. Zool.* **58**: 1992–1996.

- Sunday, J. M., A. E. Bates, and N. K. Dulvy. 2011.** Global analysis of thermal tolerance and latitude in ectotherms. *Proc. R. Soc. B Biol. Sci.* **278**: 1823–1830.
- Sunday, J., J. M. Bennett, P. Calosi, S. Clusella-Trullas, S. Gravel, A. L. Hargreaves, F. P. Leiva, W. C. E. P. Verberk, M. Á. Olalla-Tárraga, and I. Morales-Castilla. 2019.** Thermal tolerance patterns across latitude and elevation. *Philos. Trans. R. Soc. B Biol. Sci.* **374**: 20190036.
- Truebano, M., P. Fenner, O. Tills, S. D. Rundle, and E. L. Rezende. 2018.** Thermal strategies vary with life history stage. *J. Exp. Biol.* **221**: jeb171629.
- Tüzün, N., L. O. de Beeck, K. I. Brans, L. Janssens, and R. Stoks. 2017.** Microgeographic differentiation in thermal performance curves between rural and urban populations of an aquatic insect. *Evol. Appl.* **10**: 1067–1075.
- Ueda, N., and A. Boettcher. 2009.** Differences in heat shock protein 70 expression during larval and early spat development in the eastern oyster, *Crassostrea virginica* (Gmelin, 1791). *Cell Stress Chaperones* **14**: 439–443.
- Vaughn, C. C., and F. M. Fisher. 1992.** Dispersion of the salt-marsh periwinkle *Littoraria irrorata*: effects of water level, size, and season. *Estuaries* **15**: 246.
- Venables, W. N., and B. D. Ripley. 2002.** *Modern applied statistics with S*, 4th ed. Springer, New York.
- Weather Underground. 2018.** Weather Underground. [Online]. Available: <https://www.wunderground.com/history/monthly/us/fl/jacksonville/KFLPONTE55/date/2018-2>, <https://www.wunderground.com/history/monthly/us/sc/myrtle-beach/KMYR/date/2018-8>, <https://www.wunderground.com/history/monthly/us/va/newport-news/KPHF/date/2018-8> <https://www.wunderground.com/history/monthly/us/fl/jacksonville/KFLPONTE55/date/2018-8> [2020, December 14].
- Wooliver, R., S. B. Tittes, and S. N. Sheth. 2020.** A resurrection study reveals limited evolution of thermal performance in response to recent climate change across the geographic range of the scarlet monkeyflower. *Evolution* **74**: 1699–1710.
- Xiaojun, X., and S. Ruyung. 1990.** The bioenergetics of the southern catfish (*Silurus meridionalis* Chen). I. Resting metabolic rate as a function of body weight and temperature. *Physiol. Zool.* **63**: 1181–1195.

Appendix

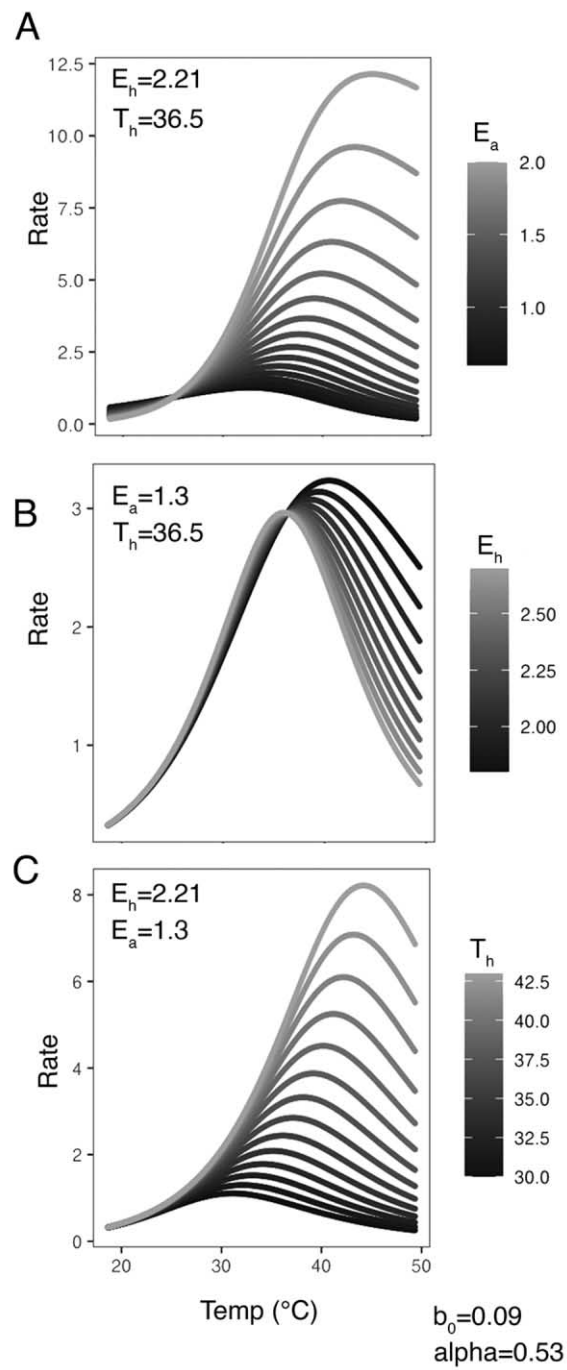


Figure A1. Estimated thermal performance curves for *Littoraria irrorata* using Sharpe-Schoolfield model parameter estimates. Parameter ranges were chosen based on a null model fit to the respiration experiment data and span the upper and lower 95% confidence intervals of the fitted thermal trait parameters (A) activation energy (E_a), (B) deactivation energy (E_h), and (C) the temperature at which half the enzymes are no longer functional (T_h) (equation 2). b_0 represents the respiration rate of a 1-unit mass individual at a reference temperature (T_c); α is the mass-scaling exponent.

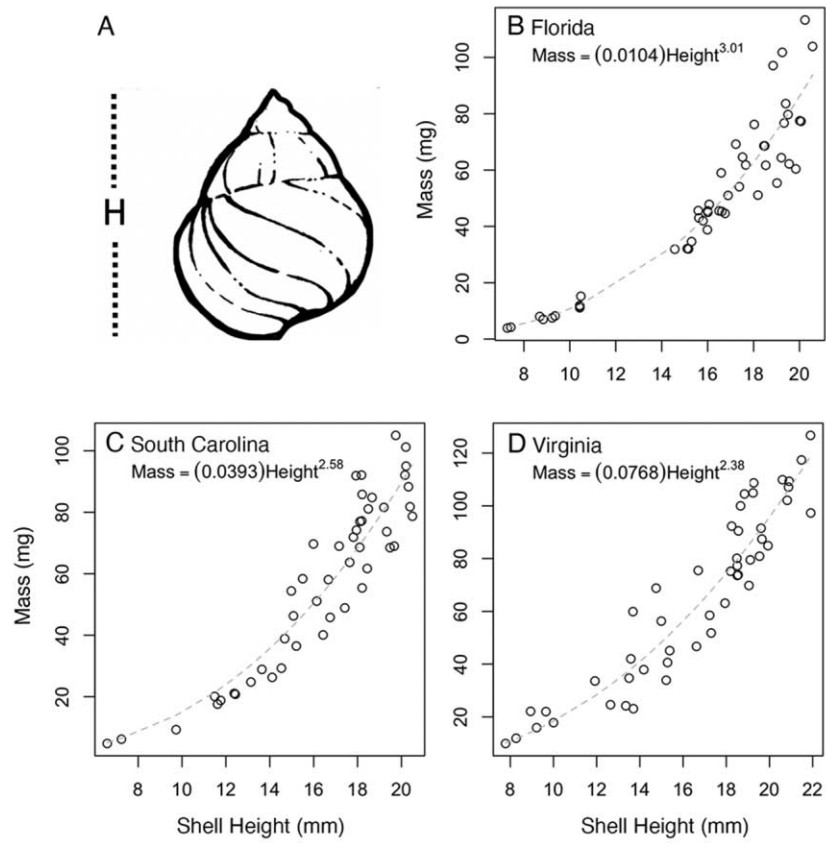


Figure A2. Creating site-specific regressions for *Littoraria irrorata*. (A) Diagram of *Littoraria irrorata* depicting shell height (H). Shell height-dry mass regressions for *L. irrorata* for three study sites: (B) Florida, (C) South Carolina, and (D) Virginia. Dry mass (mg) is measured with the shell removed but operculum intact.

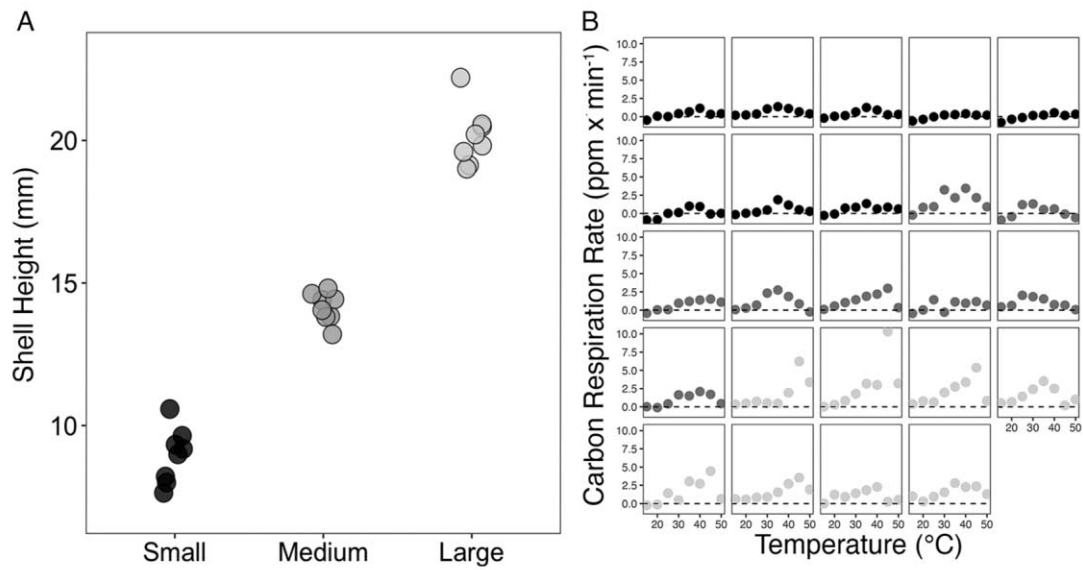


Figure A3. Visualizing differences across treatments within the respiration experiment. (A) Shell height (mm) of all individual *Littoraria irrorata* used in the respiration experiment. Shades represent size classes of individual snails (black indicates small, dark gray indicates medium, and light gray indicates large). Horizontal skew is to aid in visualizing the individual points. (B) Respiration rates (CO_2 ppm min^{-1}) for each snail (*L. irrorata*) at the eight assay temperatures ($^{\circ}\text{C}$). Shades represent size classes of individual snails (light gray indicates large, dark gray indicates medium, and black indicates small). Each rate was calculated during the final 15 minutes of each 30-minute period.

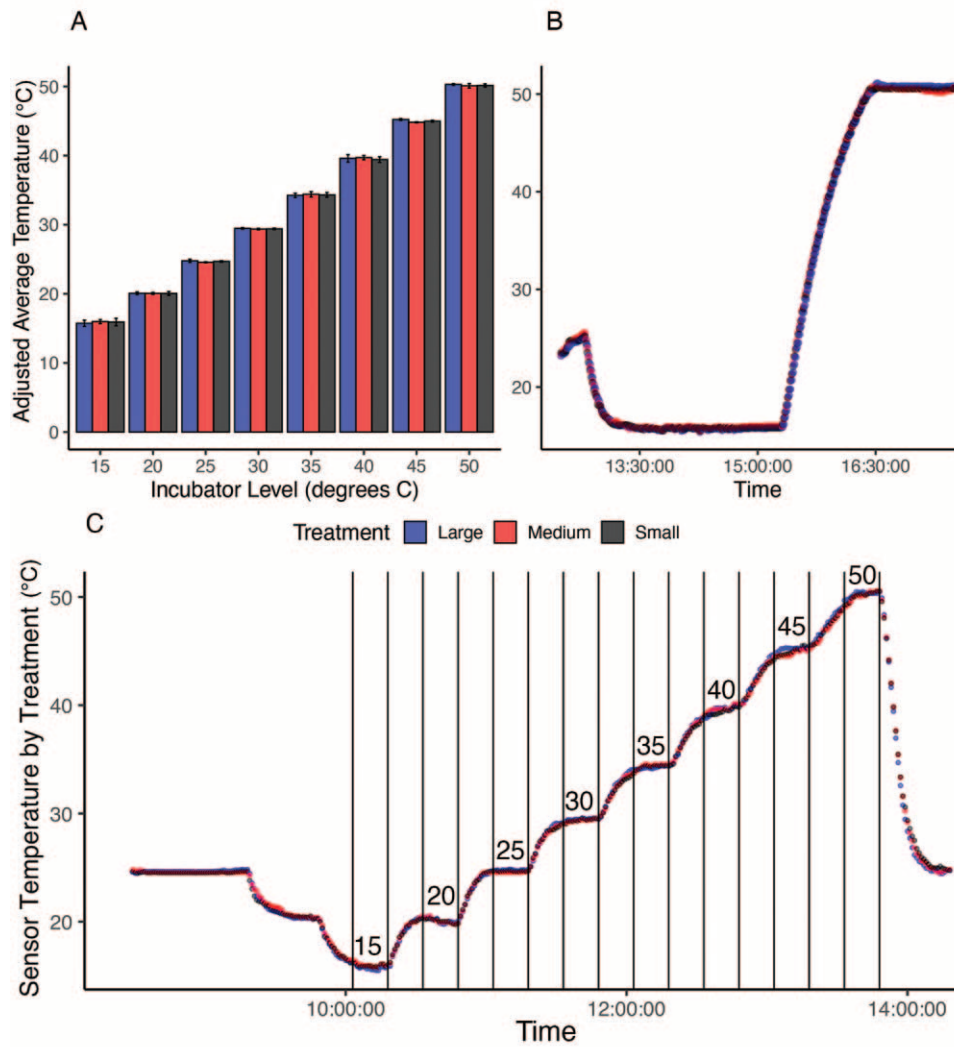


Figure A4. Temperature changes for each of the three size classes of *Littoraria* snail. (A) The temperature of snails during the final 15 minutes at each temperature was invariant across size classes and equal to the treatment temperature. In (B), snails responded similarly to a severe temperature change from 15 to 50 °C. In (C), temperature changes mirrored those imposed in the respiration experiment. The vertical lines are drawn every 15 minutes, with the final 15 minutes at each temperature indicated by the inserted numbers that give the treatment temperature. Therefore, we restricted our analyses to respiration measured during the final 15-minute window when temperatures were relatively constant.

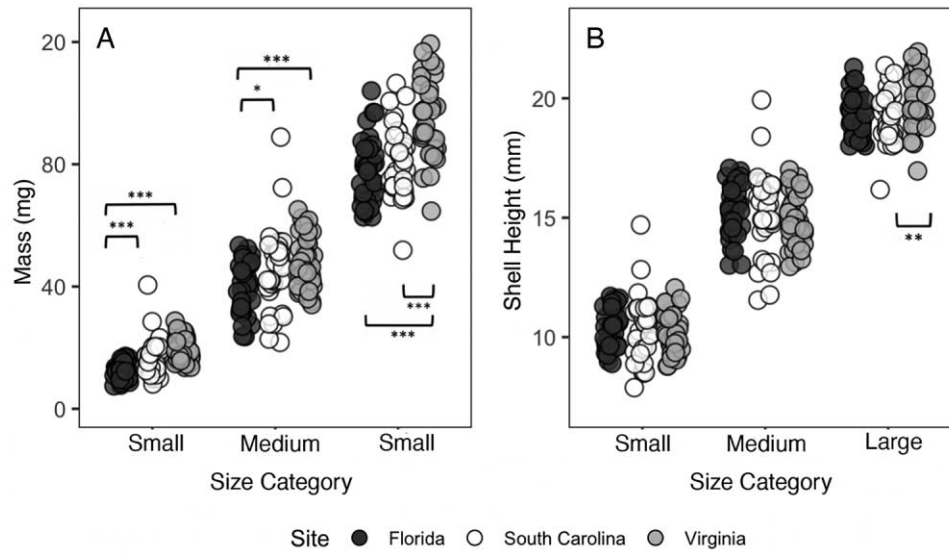


Figure A5. Visualizing differences across treatments within the feeding experiment. (A) Shell-free dry biomass (mg) and (B) shell height (mm) of all *Littoraria irrorata* individuals used in the feeding experiment. Significant differences between sites are noted (* $P < 0.05$, ** $P < 0.01$, *** $P < 0.001$). Shades represent sites (dark gray indicates Florida, white indicates South Carolina, and light gray indicates Virginia). Horizontal skew is added to aid in visualizing the individual points.

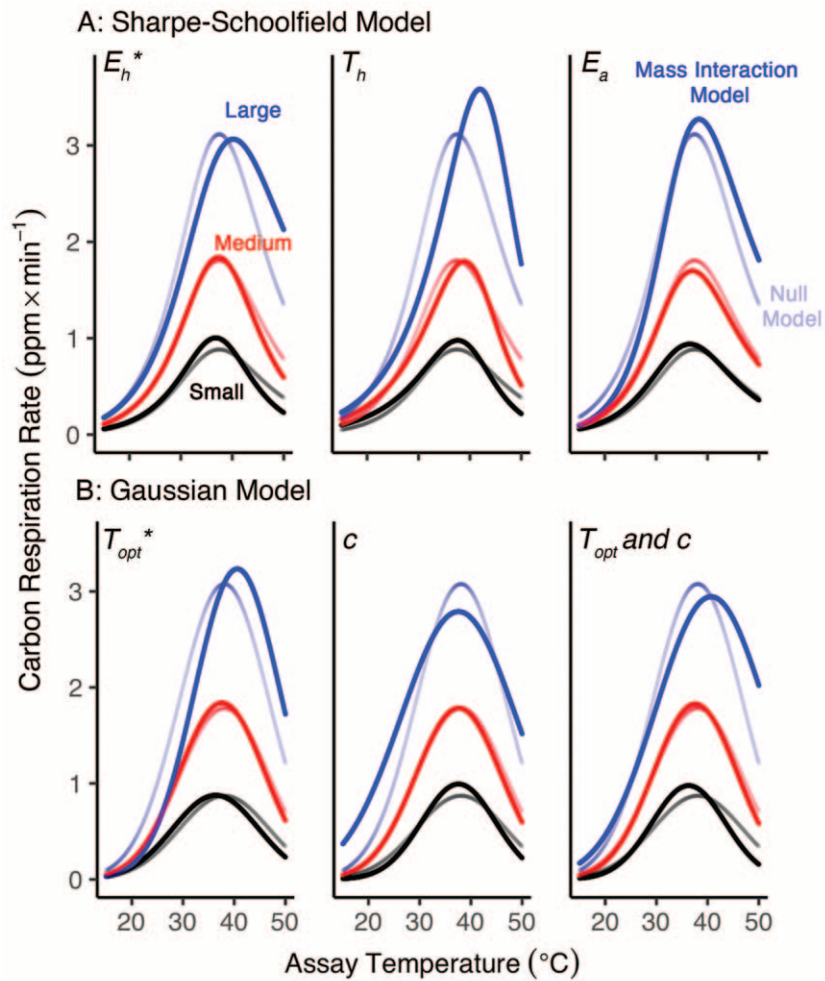


Figure A6. Predicted thermal performance curves (TPCs) for respiration rate ($\text{CO}_2 \text{ ppm min}^{-1}$). These figures illustrate how TPCs for the respiration rate of *Littoraria irrorata* change for a large (86.28 mg), medium (30.87 mg), and small (8.01 mg) snail when each thermal trait (activation energy [E_a], deactivation energy [E_h], and temperature at which half the enzymes are no longer functional [T_h] for Sharpe-Schoolfield; temperature at which a respiration rate is maximal [T_{opt}] and the parameter controlling the width of the thermal performance curve [c] for the Gaussian model) is mass dependent relative to a null model in which the thermal traits are independent of mass. The curves for the null model are identical in the three panels for the (A) Sharp-Schoolfield and (B) Gaussian model, and the two panels with an asterisk denote the most parsimonious model fit for each model.

Table A1*Design of the respiration experiment*

Time	T (°C)	Trial	March 1	March 2	March 3	March 4	March 5	March 6	March 7	March 8
			Snail size (ID)							
7:30	(25)	1	Large (1)	Small (4)	Small (8)	Medium (12)	Small (15)	Medium (18)	Small (21)	Large (22)
8:00	(20)									
8:30	15									
9:00	20									
9:30	25									
10:00	30									
10:30	35									
11:00	40									
11:30	45									
12:00	50									
12:30	(25)	2	Medium (2)	Large (5)	Large (9)	Small (11)	Medium (13)	Large (16)	Medium (19)	Small (24)
13:00	(20)									
13:30	15									
14:00	20									
14:30	25									
15:00	30									
15:30	35									
16:00	40									
16:30	45									
17:00	50									
17:30	(25)	3	Small (3)	Medium (6)	Medium (7)	Large (10)	Large (14)	Small (17)	Large (20)	Medium (23)
18:00	(20)									
18:30	15									
19:00	20									
19:30	25									
20:00	30									
20:30	35									
21:00	40									
21:30	45									
22:00	50									
22:30	25									

Littoraria irrorata ID is shown in parentheses. Data were collected only during the final 15 minutes of each 30-minute period beginning at 15 °C. The initial 2 temperature blocks (25 °C and 20 °C) were excluded from all analyses.

Table A2

Model comparisons to assess mass dependency in thermal traits, using the Sharpe-Schoolfield model fit to the data from the respiration experiment for Littoraria irrorata

Mass dependency	K	AIC _c	Δ AIC _c	BIC	Δ BIC
E_h	8	436.24	0.00	461.51	0.00
T_h	8	437.82	1.58	463.10	1.58
E_h, T_h	9	437.34	1.10	465.67	4.15
E_a, T_h	9	437.50	1.26	465.83	4.32
E_a, E_h	9	437.65	1.41	465.98	4.47
None (null model)	7	444.17	7.93	466.37	4.85
E_a	8	442.63	6.39	467.90	6.39
E_a, E_h, T_h (full model)	10	439.31	3.07	470.67	9.16

The best-fitting model included mass dependency of E_h , with Δ AIC_c (Akaike information criterion for small sample sizes) and Δ BIC (Bayesian information criterion) calculated relative to that best model. K gives the number of parameters in the model. The dataset consists of 192 estimates of respiration rates (CO₂ ppm min⁻¹). E_a , activation energy; E_h , deactivation energy; T_h , temperature at which half the enzymes are no longer functional.

Table A3

Parameter estimates (and 95% confidence intervals) of the most parsimonious Sharpe-Schoolfield model fit to the data from the respiration experiment for *Littoraria irrorata* (n = 192)

Parameter	Estimate	Lower 95% CI	Upper 95% CI
b_0	0.12	0.055	0.18
α	0.45	0.32	0.59
E_a	1.20	0.67	1.74
T_h	37.4	32.7	42.2
E'_h	2.77	2.06	3.48
β_{E_h}	-0.011	-0.020	-0.0014

Mass dependency of E_h in the Sharpe-Schoolfield model was modeled as a linear function of mass ($E_h = E'_h + \beta_{E_h}M$, in which E'_h [the downward slope at a dry tissue mass of 0 mg] gives the estimated intercept and β_{E_h} (the linear change in E_h with a 1-mg change in dry tissue mass) gives the slope (*i.e.*, the effect of mass on the parameter). α , mass-scaling exponent; b_0 , the respiration or feeding rate of a 1-unit mass individual at a reference temperature (T_c); CI, confidence interval; E_a , activation energy; T_h , temperature at which half the enzymes are no longer functional.

Table A4

Model comparisons to assess mass dependency in thermal traits, using the Sharpe-Schoolfield model fit to the data from the feeding experiment for *Littoraria irrorata*

Mass dependency	Temperature dependency	K	AIC _c	Δ AIC _c	BIC	Δ BIC
Florida						
Null model	None	7	18.88	0.00	36.30	0.00
None	α	8	20.45	1.58	40.18	3.88
E_h	None	8	20.58	1.70	40.31	4.01
T_h	None	8	20.85	1.97	40.58	4.28
E_a	None	8	21.12	2.25	40.86	4.56
E_h, T_h	None	9	19.83	0.95	41.82	5.52
E_a, T_h	None	9	19.84	0.96	41.83	5.53
E_a, E_h	None	9	22.39	3.51	44.38	8.08
E_a, E_h, T_h	None	10	22.02	3.14	46.22	9.92
South Carolina						
T_h	None	8	-149.81	0.35	-130.08	0.00
Null model	None	7	-147.31	2.85	-129.89	0.19
E_a, E_h	None	9	-149.58	0.57	-127.59	2.48
E_a	None	8	-146.14	4.02	-126.41	3.67
E_h, T_h	None	9	-148.16	2.00	-126.16	3.91
E_a, E_h, T_h	None	10	-150.16	0.00	-125.96	4.12
E_a, T_h	None	9	-147.94	2.21	-125.95	4.12
E_h	None	8	-145.43	4.72	-125.70	4.37
T_h	α	9	-147.43	2.73	-125.44	4.64
Virginia						
Null model	None	7	39.15	2.11	56.58	0.00
T_h	None	8	39.25	2.21	58.98	2.41
E_a, T_h	None	9	37.04	0.00	59.03	2.46
E_h	None	8	39.87	2.82	59.60	3.02
E_h, T_h	None	9	38.03	0.99	60.02	3.45
E_a, T_h	None	9	38.41	1.37	60.40	3.82
E_a	None	8	41.49	4.45	61.22	4.65
None	α	8	41.49	4.45	61.22	4.65
E_a, E_h, T_h	None	10	39.48	2.44	63.68	7.10

Data from each of the three sites were fit separately ($n = 105$ snails per site). The best-fitting model for two of the three sites was the null model, which lacked mass dependency; Δ AIC_c (Akaike information criterion for small sample sizes) and Δ BIC (Bayesian information criterion) are calculated relative to the best model. K gives the number of parameters in each model. α , mass-scaling exponent; E_a , activation energy; E_h , deactivation energy; T_h , temperature at which half the enzymes are no longer functional.

Table A5

Parameter estimates (and 95% confidence intervals) from the Sharpe-Schoolfield model fit to the data from the feeding experiment for Littoraria irrorata

Parameter	Site	Estimate	Lower 95% CI	Upper 95% CI
b_0	FL	0.0122	-0.00738	0.0317
	SC	0.00059	-0.000883	0.00206
	VA	0.00111	-0.000503	0.00273
α	FL	1.14	0.91	1.37
	SC	1.81	1.49	2.13
	VA	1.74	1.49	1.98
E_a	FL	0.68	-0.68	2.04
	SC	1.04	-1.07	3.15
	VA	1.09	-0.15	2.33
E_h	FL	1.40	0.69	2.11
	SC	1.70	0.13	3.27
	VA	1.71	0.86	2.56
T_h	FL	28.6	6.7	50.6
	SC	23.6	8.5	38.7
	VA	27.1	15.9	38.2

The model does not include any effect of mass on the thermal traits or temperature on mass scaling and was applied separately to each of the three study populations (Florida [FL], South Carolina [SC], and Virginia [VA]). $n = 105$ snails per site. The best Sharpe-Schoolfield model for SC included the mass dependency of T_h ; however, a difference in BIC values of less than 2 suggests that these models are indistinguishable ($\Delta AIC_c = -2.5$ and $\Delta BIC = -0.19$). α , mass-scaling exponent; AIC_c , Akaike information criterion for small sample sizes; b_0 , the feeding rate of a 1-unit mass individual at a reference temperature (T_c); BIC, Bayesian information criterion; E_a , activation energy; E_h , deactivation energy; T_h , temperature at which half the enzymes are no longer functional.